UJEAS

UNIZIK JOURNAL OF ENGINEERING AND APPLIED SCIENCES

UNIZIK Journal of Engineering and Applied Sciences 3(1), March (2024), 457-478
Journal homepage: https://journals.unizik.edu.ng/index.php/ujeas
PRINT ISSN: 2992-4383 || ONLINE ISSN: 2992-4391

Fault Diagnosis on a 330kV Power System Transmission Line Using S-Transform Technique

Ojukwu, A.C.*, Onuegbu, J.C. and Ogboh, V.C.
Department of Electrical Engineering, Nnamdi Azikiwe University, Awka, Nigeria.
*Corresponding Author's E-mail: ojukwualbert@yahoo.com

Abstract
Due to the frequent and unpredictable occurrence of faults in the power transmission system, the need for a method intelligent enough to detect and diagnose faults becomes imminent to ensure the reliability of power system protection. This paper presents a fault diagnosis approach that uses the S-Transform technique to detect and analyze the fault occurring on the 330kV Ajaokuta to Lokoja 47.39km transmission line using MATLAB/SIMULINK. The S-Transform technique modelled, employs a scalable and moving localizing Gaussian window to identify faults. The voltage and current energy signal, the S-transform waveform, and the discrete voltage and current signal are used to diagnose each fault condition simulated on the line. The results obtained shows that at pre-fault condition, the value of the voltage magnitude was greater than the value of the current magnitude while at various fault conditions, the value of the current magnitude was greater than the value of the voltage magnitude which were all in accordance with conventional circuit theorem.

Keywords: S-Transform, Transmission line, Signal, Waveform.

1. Introduction

The transmission line is an essential part of the electrical power system through which generated power is transferred to the consumers. Providing uninterrupted power to end consumers is a challenge for grid operators. Although the intrusion of faults is beyond human control, it is critical to precisely diagnose any transmission line system faults. Fault diagnosis is an area of continuous research in power system. According to Haroun, Seghir, and Tougti (2018), most electrical protection systems/relays measure current, voltage, or a combination of both in the event of a fault. In terms of the kind of fault and its position in relation to the measurement transformer, the magnitude and direction of the fault current frequently change suddenly. Symmetrical and unsymmetrical faults occur on the lines and various methods have been implemented for determination of the line conditions, type of fault that occurred and the point at which the fault occurred. Among those signal analysis method, Stockwell transform (S-Transform) is use in extracting and analyzing the features of the travelling wave. S-Transform technique has the ability to detect the disturbance correctly in the presence of noise. It is a modified version of Continuous Wavelet Transform (CWT) which retains the absolute phase of every frequency component. (Anazia, Ogboh and Anionovo, 2020).

A novel power swing detection scheme based on S-Transform together with ANN, which focusing on the transmission line protection was proposed by Mohamed, Abidin and Shareef (2014). This technique can be used to detect unstable swing with a very good accuracy but it determines the additional events of post fault which is not significantly needed to be detected in power system. Shafiullah, Abido and Al-Mohammed in "Advanced signal processing techniques (SPTs) for feature extraction", introduced the importance of STPs in analyzing power system transients. They illustrated two advanced SPTs: the discrete wavelet transforms and the Stockwell transform. After the illustration of the targeted SPT, they presented a step-by-step feature extraction process from the recorded three-phase faulty current

signals. S-transform was also used to extract useful features from the phasor measurement units (PMU) recorded current signals. The approach fetches the extracted features as inputs to the machine learning tools including the multilayer perception neural network, support vector machine and extreme learning machine to diagnose i.e., to detect, classify and locate the faults. (Shafiullah, 2022). Additionally, in "S-transform based fault detection algorithm for enhancing distance protection performance," Jose, Marjan, David, Sadegh, and Vladimir (2021) proposed a fault detection algorithm based on the Fast Discrete Stockwell Transform. This algorithm can address issues found during fault detection and improve the functionality of the current distance protection during fault occurrence in systems with high penetration of power electronics-based generators.

Among all the works reviewed, it is apparent that the S-Transform technique has not specifically been applied on distance transmission line system to diagnose faults. This paper presents a fault diagnosing scheme using S-Transform for sampling the fault voltage and current transient on the transmission line at relay point. Normally, the fault generated voltage and current transients contain long duration low frequency components and short duration high frequency components, which are employed by S-Transform for the line protection. The details on the S-Transform theory and how to employ it in the detection scheme was discussed. The 330kV Ajaokuta to Lokoja 47.39km transmission line was extracted from the MATLAB/SIMULINK Nigeria 58 bus system and used as a case study to simulated the various fault conditions which acts an input to the model S-Transform model in MATLAB/SIMULINK. The results from the detection for various fault condition were also discussed.

2.0 Material and methods

The methodology employed in carrying out the study purpose and objectives of this research article is hereby presented. The 330kv Ajaokuta-Lokoja 47.39km transmission line was extracted and modelled from the Nigerian 58-bus system in MATLAB/SIMULINK. The S-Transform equation was modelled using MATLAB/SIMULINK blocks. The model was simulated at pre-fault and various fault conditions and the fault generated voltage and current signals at various faults condition were diagnose using the voltage and current energy signal, the S-transform waveform, and the discrete voltage and current signal. The block diagram in figure 1 represents the methodological procedure for this research.

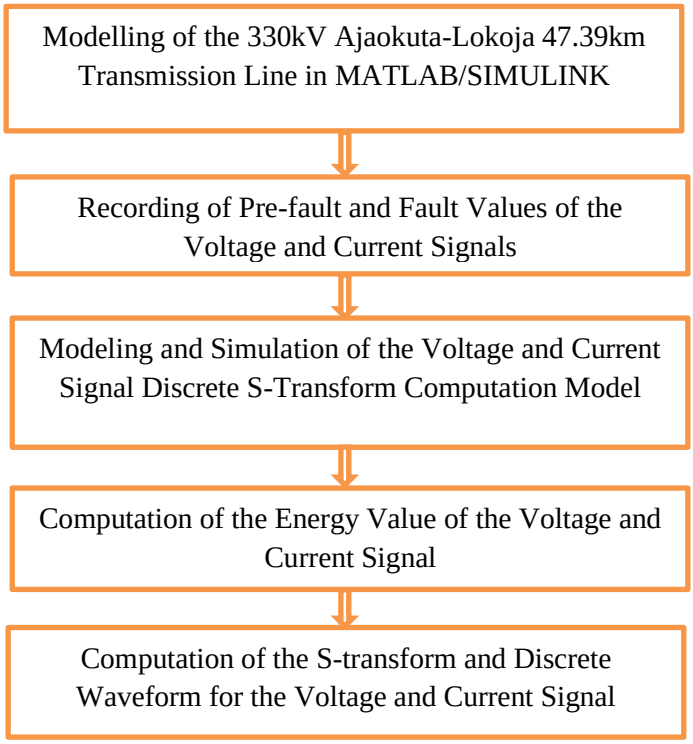

Figure 1: A Block Diagram Illustrating the Research's Methodology.

The input phase voltage ($V_a, V_b\ and\ V_c$) and phase current ($I_a, I_b\ and\ I_c$) are the input parameters to the power system network model gotten from the 330kV Ajaokuta-Lokoja 47.39km transmission line of the 58-Bus power system network as shown in Table 1.

Table 1: Pre-fault Voltage and Pre-fault Current Parameter (Input Data) Obtained from the 330kV Ajaokuta-Lokoja 47.39km Transmission Line of the 58-Bus Power System Network

Pre-Fault Voltage and Current Parameters in pu					
V_a	V_b	V_c	I_a	I_b	I_c
0.330226	-0.66065	0.330427	-0.31355	0.158394	1.55E-01
0.339173	-0.66057	0.3214	-0.31354	0.154124	0.159412
0.348036	-0.66033	0.312294	-0.31345	0.149817	0.163635
0.356813	-0.65992	0.303111	-0.31329	0.145473	0.167817
0.365503	-0.65936	0.293853	-0.31305	0.141094	0.171957
0.374102	-0.65863	0.284523	-0.31273	0.136678	0.176055
0.382609	-0.65773	0.275122	-0.31234	0.132229	0.18011
0.391022	-0.65668	0.265654	-0.31187	0.127747	0.184119
0.399338	-0.65546	0.25612	-0.31132	0.123234	0.188084
0.407555	-0.65408	0.246523	-0.31069	0.11869	0.192002
0.415672	-0.65254	0.236865	-0.30999	0.114117	0.195872
0.423687	-0.65084	0.227148	-0.30921	0.109515	0.199694
0.431597	-0.64897	0.217376	-0.30835	0.104886	0.203466
0.4394	-0.64695	0.20755	-0.30742	0.100231	0.207188
0.447095	-0.64477	0.197672	-0.30641	0.09555	0.210857
0.454679	-0.64243	0.187746	-0.30532	0.090846	0.214475
0.462152	-0.63993	0.177774	-0.30416	0.086121	0.218041

The fault voltage (V_{af}, V_{bf} and V_{cf}) and fault current ($I_{af}, I_{bf}\ and\ I_{cf}$) are the output parameters of the modelled system as shown in the Table 2 indicating the different fault conditions simulated.

Table 2: Fault Voltage and Fault Current Parameter (Output Data) of the Different Fault Simulation Obtained from the 330kV Ajaokuta-Lokoja 47.39km Transmission Line of the 58-Bus Power System Network

	Fault Voltage and Current Parameter in pu					
Condition	V_{af}	V_{bf}	V_{cf}	I_{af}	I_{bf}	I_{cf}
No Fault	0.330226	-0.66065	0.330427	-0.31355	0.158394	1.55E-01
A – G	0.3511	-0.6603	0.3091	-1.721	0.3015	0.2968
B – G	0.3801	-0.7106	0.3305	-0.1471	1.318	0.3172
C – G	3.31E-01	-0.6185	2.88E-01	0.1576	6.36E-01	-0.7676
A – B	0.2419	-0.617	0.3752	2.296	-2.447	0.1505
B – C	0.4102	-0.8198	0.4095	-0.3147	-0.5994	0.9139
C – A	0.3331	-0.6586	0.3256	2.417	0.1653	-2.583
AB – G	0.3324	-0.7272	0.3949	-0.4051	0.8533	2.7
BC – G	0.2724	-0.6411	0.3687	2.08E+00	-0.554	-0.02734
CA – G	0.4059	-0.7511	0.3452	-0.6231	-0.6858	0.3115
A – B – C	0.2425	-0.7084	0.4659	3.1	-1.644	-1.456

2.1 Modeling of the S-Transform Equation for Detection of Fault Using MATLAB/SIMULINK

Stockwell et al. (1996) presented the S-transform in "Localization of the Complex Spectrum: The S-transform," which is a variation that shows some of the desirable properties that are lacking in the continuous wavelet transform like the

ability to detect the disturbance correctly in the presence of noise. While keeping its link with the Fourier spectrum, the S-transform provides a unique frequency dependent resolution.

S-Transform of a basic continuous signal (voltage and current signal) h(t) of a transmission line is defined by the following equation;

$$S(\tau, f) = \int_{-\infty}^{\infty} h(t)\, w(f, \tau - t)\, e^{(-2\pi i f t)}\, dt \quad (1)$$

But,

$$w(f, \tau) = \frac{|F|}{\sqrt{2\pi}}\, e^{-\left(\frac{t^2}{2\alpha^2}\right)} \quad (2)$$

Where equation (2) is called the Gaussian modulating function

$$S(\tau, f) = \int_{-\infty}^{\infty} h(t) \left\{\frac{|f|}{\alpha\sqrt{2\pi}}\right\}. e^{\left(\frac{-f^2(\tau - t)^2}{2\alpha^2}\right)}. e^{(-2\pi i f t)}\, dt \quad (3)$$

Combining equation (1) and (2), we obtain equation (3)

Where f is the frequency in hertz, t is the time in seconds, and τ is the time location in seconds also known as the parameter determining the position of the Gaussian window on the t-axis and α is the standard deviation, which functions as a control factor for the transform's time and frequency resolution. Lower α values correspond to lower frequency and better temporal resolution, and vice versa.

A reasonable value for α falls between 0.2 and 1.

Equation (4) provides the discrete S-transform DST expression while taking the discrete form of the continuous S-Transform into consideration.

$$S(j, n) = \sum_{m=0}^{N-1} H(m + n). e^{\left(\frac{-2\pi^2 m^2 \alpha^2}{n^2}\right)}. e^{(i2\pi m j)} \quad (4)$$

Where, j = 1 … N-1, n = 0, 1 … N-1. But the time samples and frequency step are indicated by j and n respectively.

Next, the S-Transform yields the signal's energy E, which is as

$$E = \{abs(S(j, n_1))\}^2 \quad (5)$$

The energy signal that you acquire from the S-Transform is used for the identification and classification of the transmission line fault. (Anazia, Ogboh and Anionovo, 2020, Iwuamadi, Ezechukwu and Ogboh, 2022).

The DST S-Transform equation from (4) was modelled in MATLAB/SIMULINK for the voltage and current signal and the result model is shown in Figures 3 and 4.

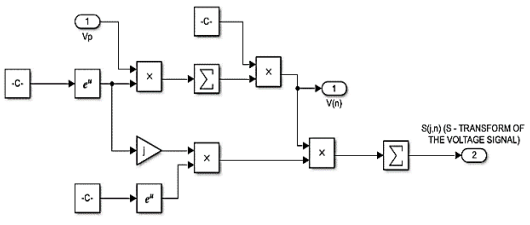

Figure 2: The S-Transform Discrete Model for Current Signal.

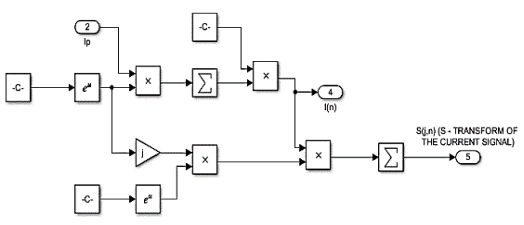

Figure 3: The S-Transform Discrete Model for Voltage Signal.

The discrete energy signal of voltage and current is the signal that depicts the magnitude, severity, and frequency of line faults. Conventional theories of networks or circuits state that when a fault arises in an electrical circuit, the magnitude of the voltage drops and the magnitude of the current rises. Consequently, the voltage energy signal's amplitude can only exceed the current energy signal's size in the absence of fault in the network. It is expected that the voltage energy signal would be less than the current energy signal when a fault occurs in the network. If, following fault simulations, the voltage energy signal output is larger than the current energy signal output, the energy equation of 5 is not true (Iwuamadi et al., 2022).

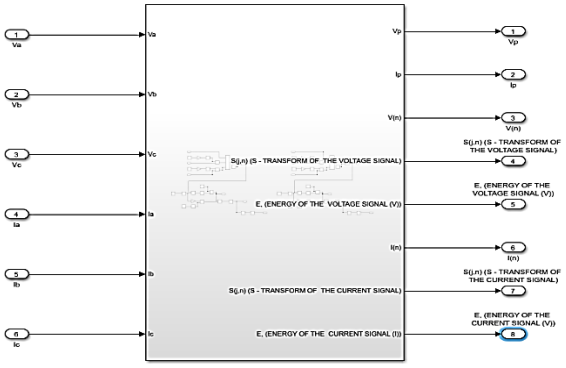

Figure 4: The Discrete S-Transform Model for the Voltage and Current Signal: A Comprehensive MATLAB/SIMULINK Subsystem.

The MATLAB/SIMULINK subsystem model is used to compute the discrete values of the voltage and current during pre-fault and fault conditions, as well as the energy models for the voltage and current signal and the S-Transform fault detection model, as shown in Figure 4. The output of the MATLAB/SIMULINK voltage-current measurement block is linked to the inputs of the S-Transform fault detection model to extract the phase voltage and current signals, which are then evaluated using the mathematical model. The outcome is provided to demonstrate whether there is a fault or not.

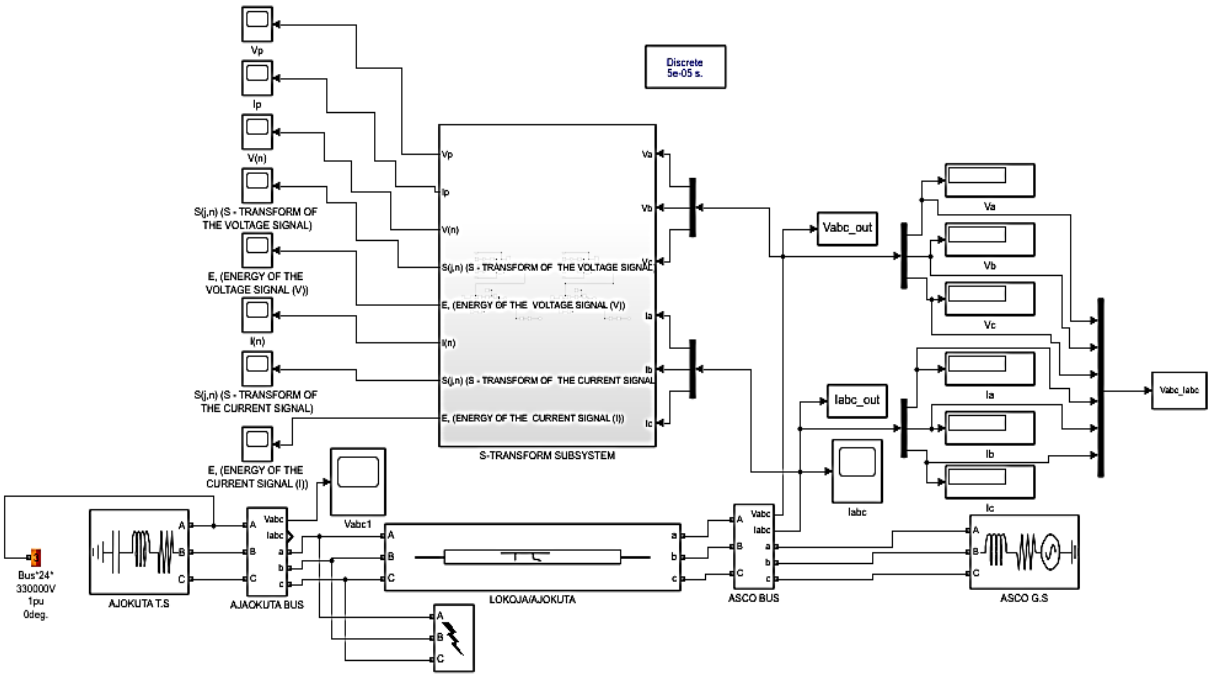

Figure 5: The MATLAB/SIMULINK Model Used for the Fault Diagnosis of the 330 kV Ajaokuta to Lokoja 47.39km Transmission Line Network Using S-Transform.

3.0 Results and Discussions

The results covered the finding from the fault diagnosis of the Nigerian 58-Bus network using a case study of the 330kV Ajaokuta-Lokoja 47.39 km transmission line. The outcomes were obtained using the approach that this study described. The following conclusions were reached as a result of simulating the Simulink model for the fault diagnostics for the different fault conditions.

i. At Pre-fault Condition

Figure 6 depicts the pre-fault voltage waveform of the system after modeling it with no fault. When there is no fault in the system, the three-phase voltage waveform moves in a uniform sinusoidal shape. The magnitude of the three-phase gaussian window width looks to be 0.65pu. Figure 7 depicts the pre-fault current wave of the system under consideration. Because there is no fault current in the system, the magnitude of the current for each phase is relatively the same at 0.3pu smaller than the value of the voltage at 0.65pu.

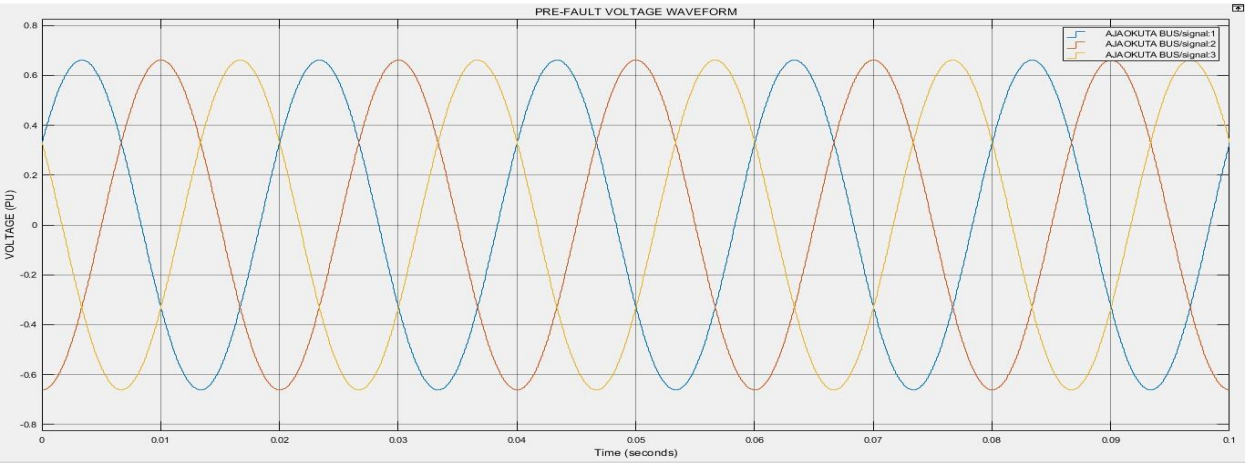

Figure 6: Pre-fault Voltage Waveform for the System Modelled.

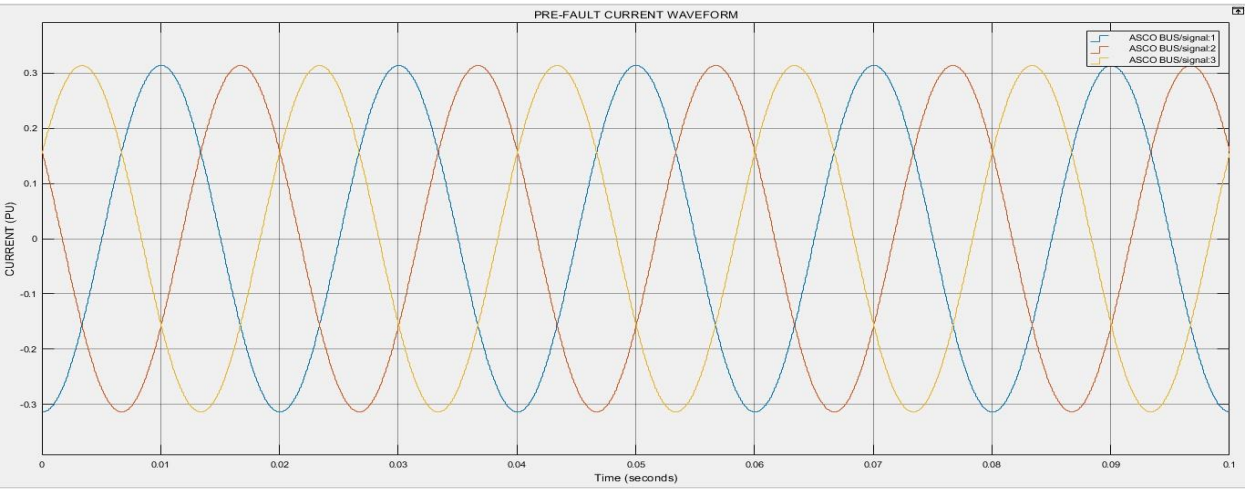

Figure 7: Pre-fault Current Waveform for the System Modelled.

Figure 8 depicts the energy of the voltage signal in the pre-fault situation. The magnitude of the voltage energy signal obtained from the S-transform model is $1.6947x10^{27}J$, with a constant gaussian waveform throughout the plane. Figure 9 shows that the energy of the current signal, derived from the S-transform model, is $1.2725x10^{26}J$. Since there is no fault in the system, the magnitude of the energy of the voltage signal at $1.6947x10^{27}J$ is larger than that of the energy of the current signal.

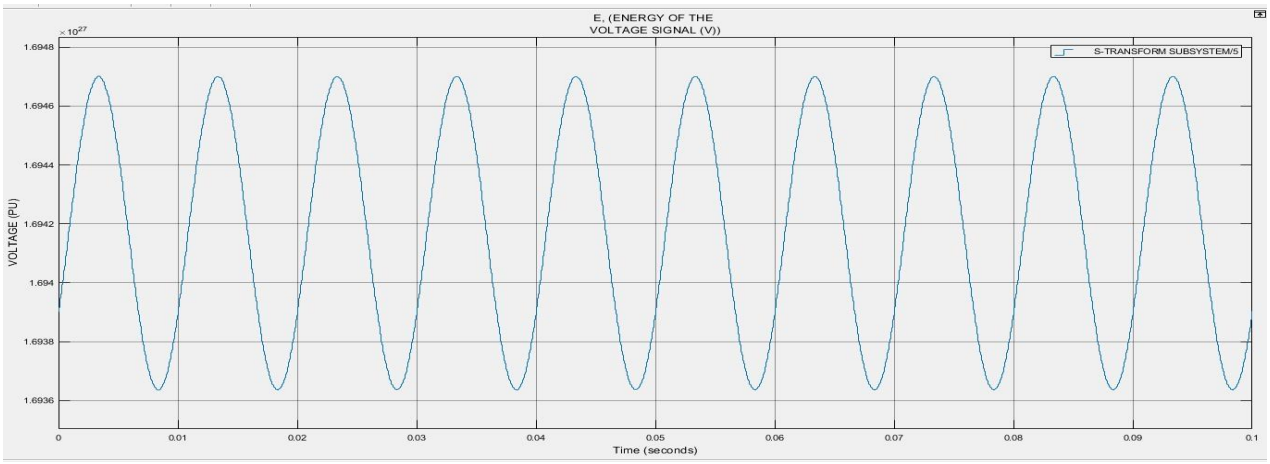

Figure 8: The Voltage Signal Energy Waveform during Pre-fault Condition.

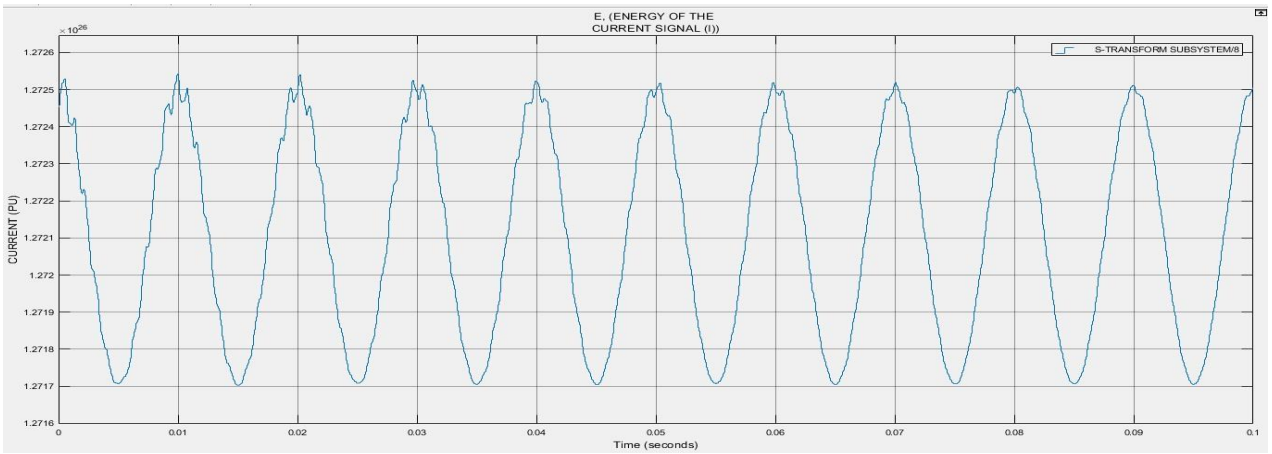

Figure 9: The Current Signal Energy Waveform during Pre-fault Condition.

Figure 10 depicts the S-transform waveform of the voltage signal in the pre-fault situation. The magnitude of the voltage S-transform signal obtained from the S-transform model is $4x10^{13}$, with a constant gaussian waveform throughout the plane. Figure 11 shows that the S-transform waveform of the current signal obtained from the S-transform model is $1x10^{13}$. Since there is no fault in the system, the magnitude of the S-transform voltage signal at $4x10^{13}$ is larger than that of the S-transform of the current signal.

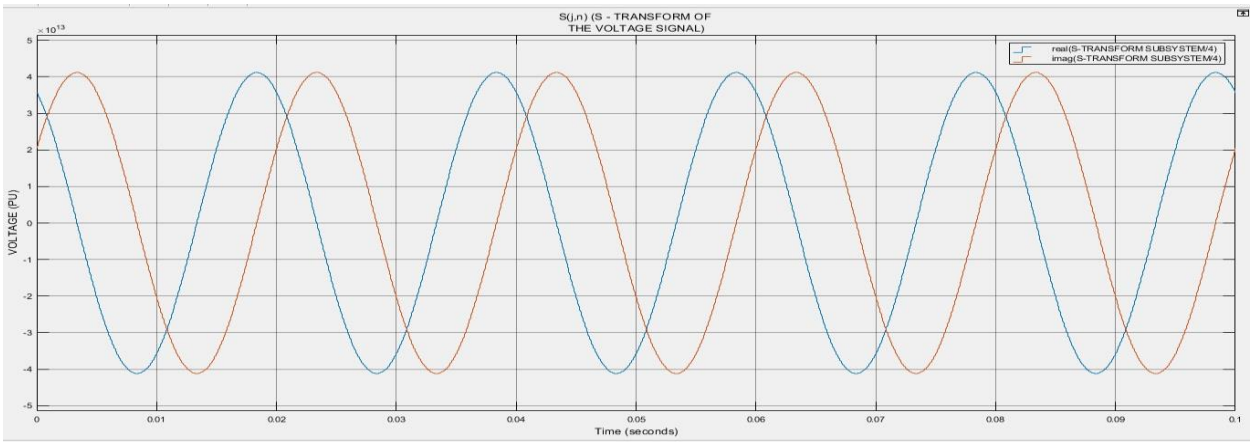

Figure 10: The S-transform of the Voltage Signal during Pre-fault Condition.

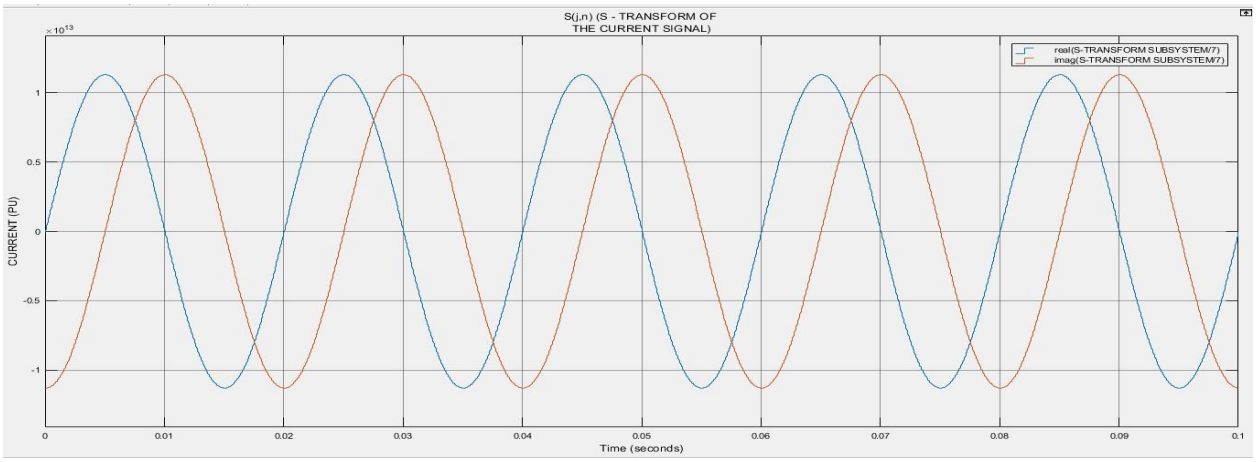

Figure 11: The S-transform of the Current Signal during Pre-fault Condition.

Figure 12 depicts the discrete voltage signal in the pre-fault situation. The magnitude of the discrete voltage signal obtained from the S-transform model is 1.0pu, with a constant gaussian waveform throughout the plane. Figure 13 shows that the discrete current signal obtained from the S-transform model is 0.3pu. Since there is no fault in the system, the magnitude of the discrete voltage signal at 1pu is larger than that of the discrete value of the current signal.

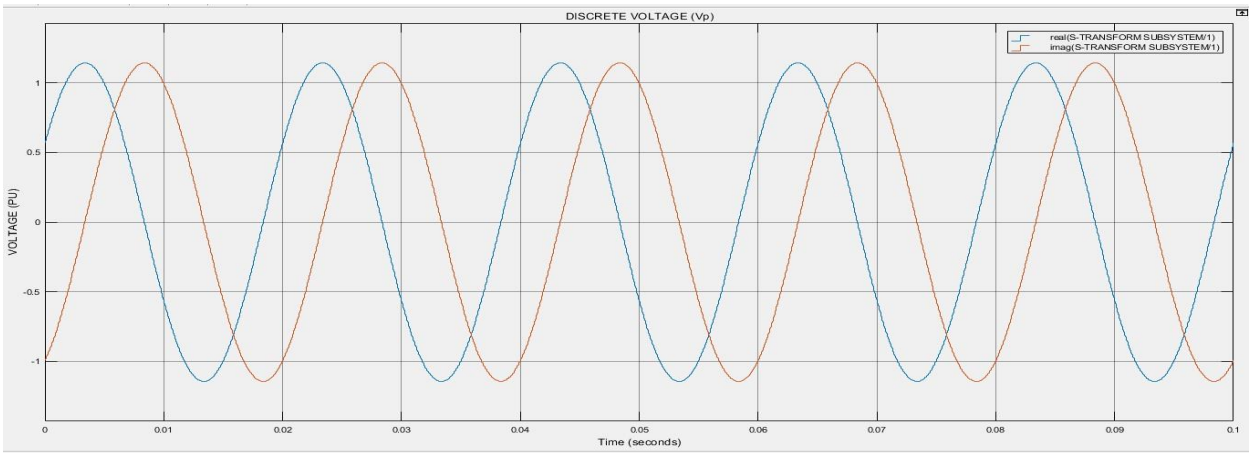

Figure 12: The Discrete Voltage Signal during Pre-fault Condition.

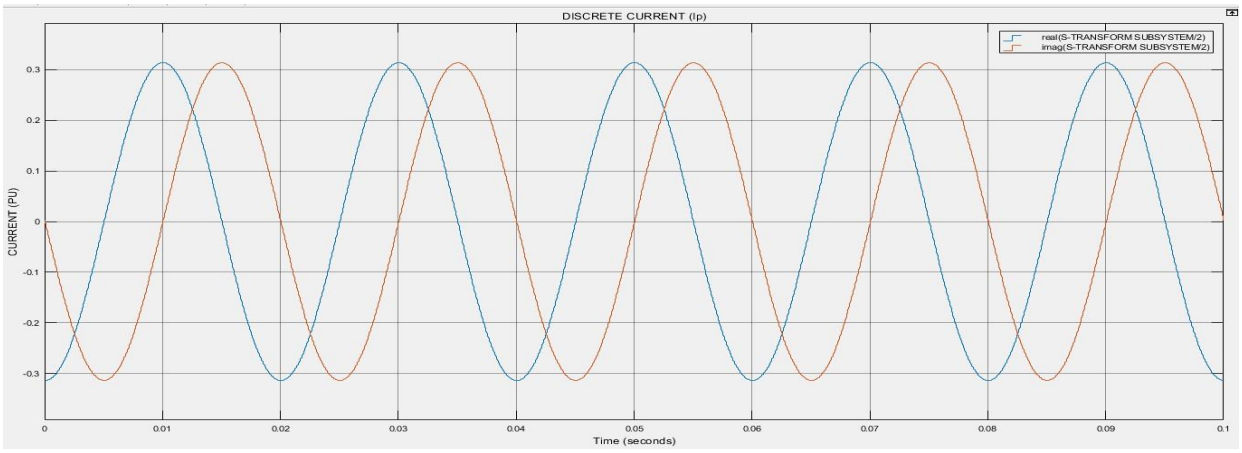

Figure 13: The Discrete Current Signal during Pre-fault Condition.

Table 3: The Result Obtained at No Fault Condition

S/N	PARAMETER	MAGNITUDE (PU)
1	Voltage (V)	0.65
2	Current (I)	0.3
3	Energy of the voltage signal E_j (J)	$1.6947x10^{27}J$
4	Energy of the current signal E_j (J)	$1.2725x10^{26}$
5	S-transform of the voltage signal	$4x10^{13}$
6	S-transform of the current signal	$1x10^{13}$
7	Discrete voltage signal	1.0
8	Discrete current signal	0.3

ii. At Single Phase to Ground Fault

The following data were obtained when a single phase to ground fault was simulated on the system, say on phase A, B, or C, at a time of 17msecs and persisted until it was cleared at 85msecs, which lasted roughly 68msecs.

During fault simulation, a spike was seen in the defective phase. The magnitude of the current in the defective phase grew to around 40pu for the single phase to ground, while the current in the remaining healthy phases remained unchanged. After the fault is resolved, the amplitude of the defective phase's current becomes uniform with the size of the remaining healthy phases' current. Figures 15 shows the current waveform.

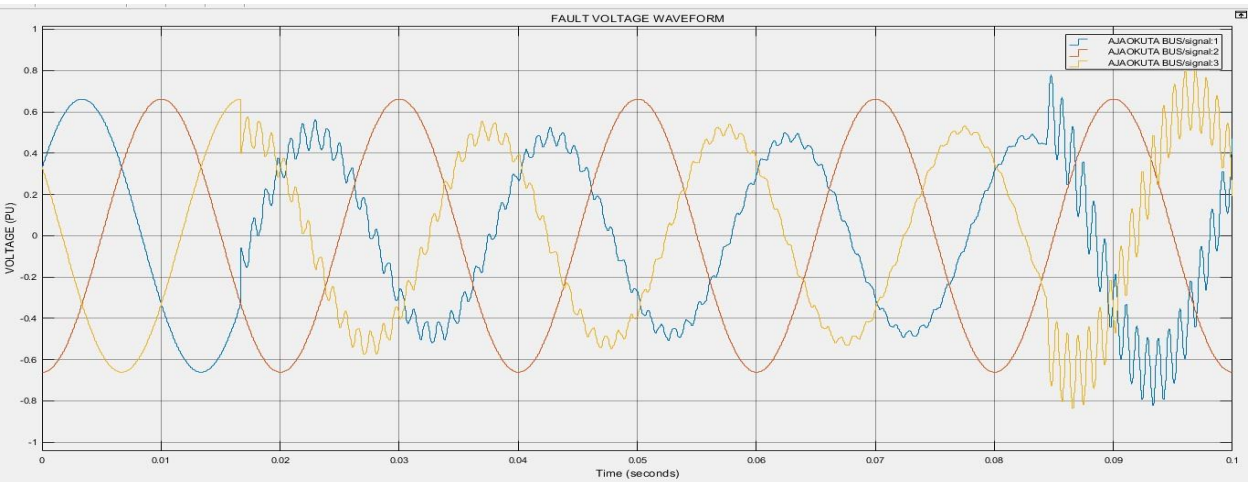

Figure 14: Single Phase to Ground Fault Voltage Waveform for the System Modelled.

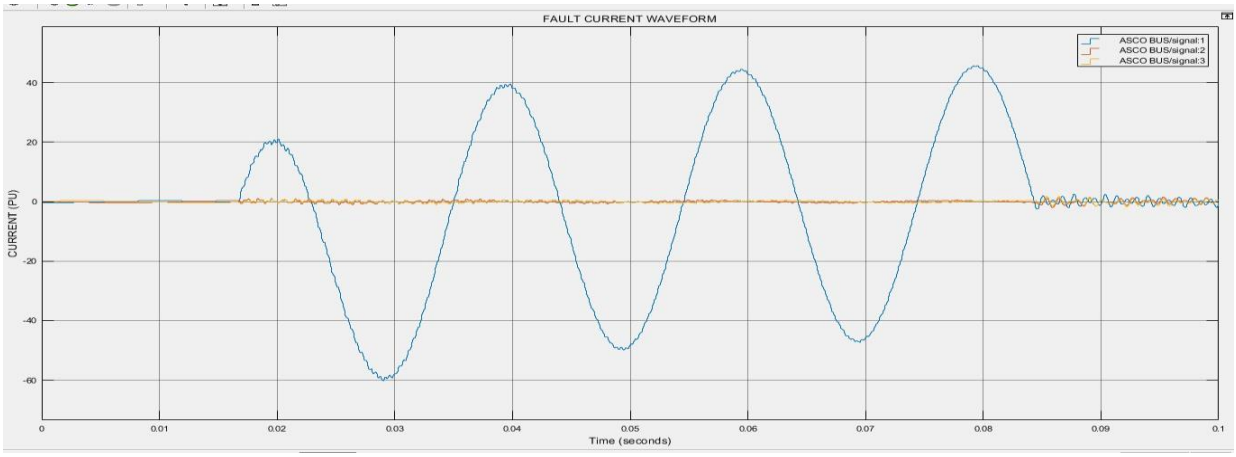

Figure 15: Single Phase to Ground Fault Current Waveform for the System Modelled.

Furthermore, the magnitude of the voltage energy signal from the S-Transform model in figure 16 gets distorted at $1.7x10^{27}J$ during the fault condition, which is now smaller than the magnitude of the current energy signal in figure 17 at $2.0x10^{30}J$. When the fault occurs at 17msecs, the current energy signal magnitude spikes to $2.0x10^{30}J$ and is recovered once the fault is cleared at 85msecs.

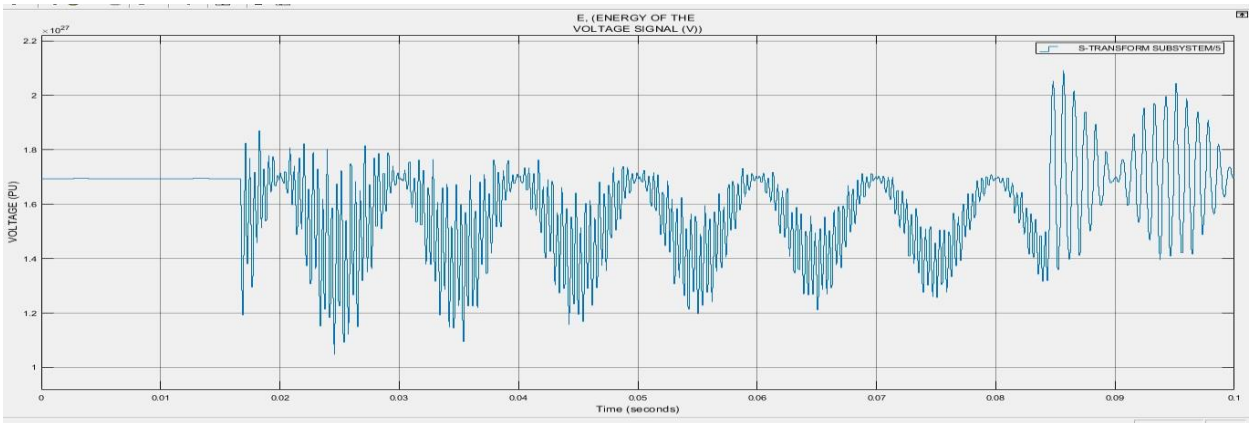

Figure 16: The Voltage Signal Energy Waveform during Single Phase to Ground Fault Condition.

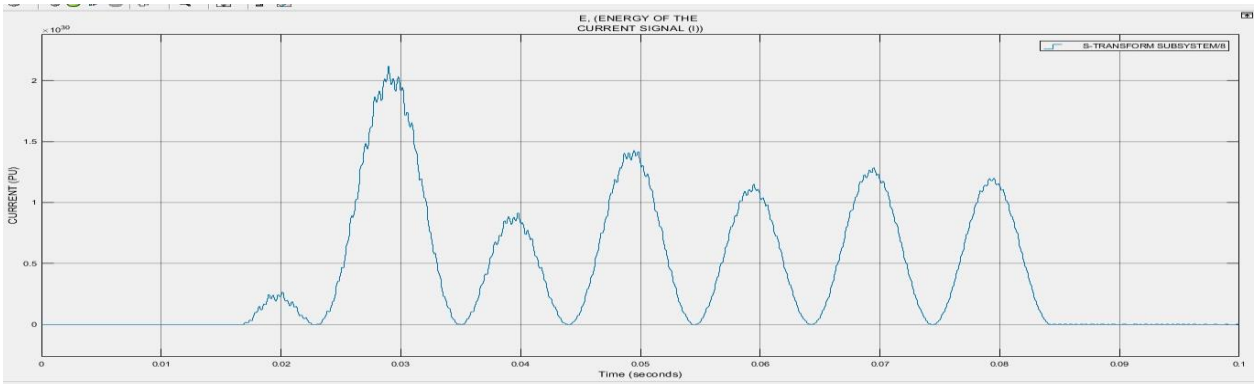

Figure 17: The Current Signal Energy Waveform during Single Phase to Ground Fault Condition.

Still also, the S-transform magnitude of the voltage signal from the S-Transform model in figure 18 gets distorted at $4x10^{13}$ during the fault condition, which is now smaller than the magnitude of the S-transform of the current signal in figure 19 at $1x10^{15}$. When the fault occurs at 17msecs, the current signal magnitude spikes to $1x10^{15}$ and is recovered once the fault is cleared at 85msecs.

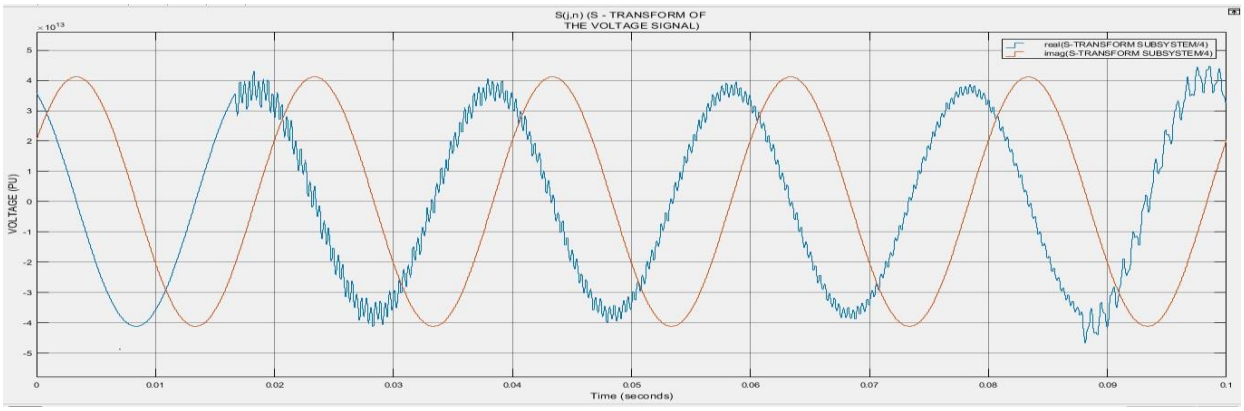

Figure 18: The S-transform of the Voltage Signal during Single Phase to Ground Fault Condition.

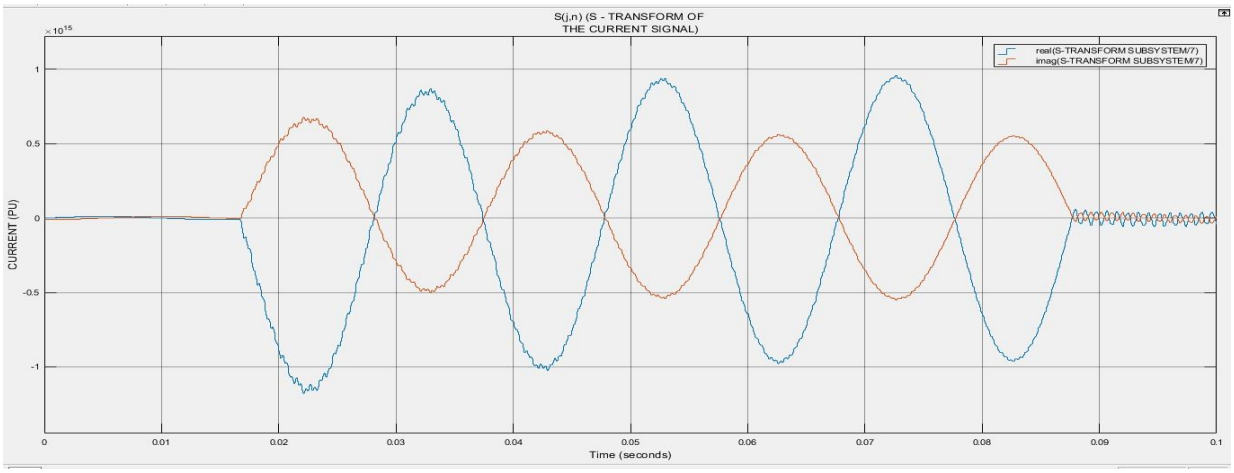

Figure 19: The S-transform of the Current Signal during Single Phase to Ground Fault Condition.

Finally, the discrete value of the voltage signal from the S-Transform model in figure 20 gets distorted at 1.0pu during the fault condition, which is now smaller than the discrete value of the current signal in figure 21 at 20pu. When the fault occurs at 17msecs, the current signal magnitude spikes to 20pu and is recovered once the fault is cleared at 85msecs.

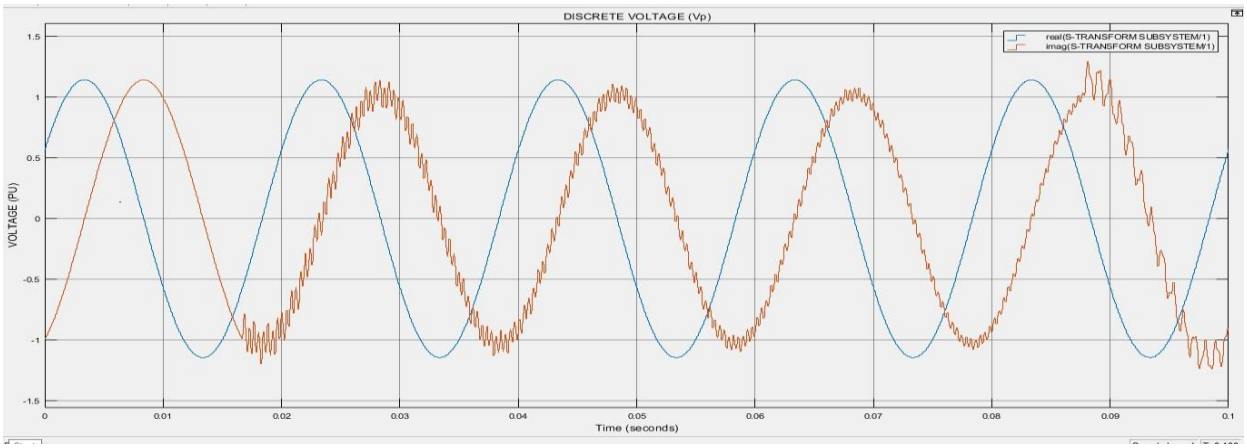

Figure 20: The Discrete Voltage Signal during Single Phase to Ground Fault Condition.

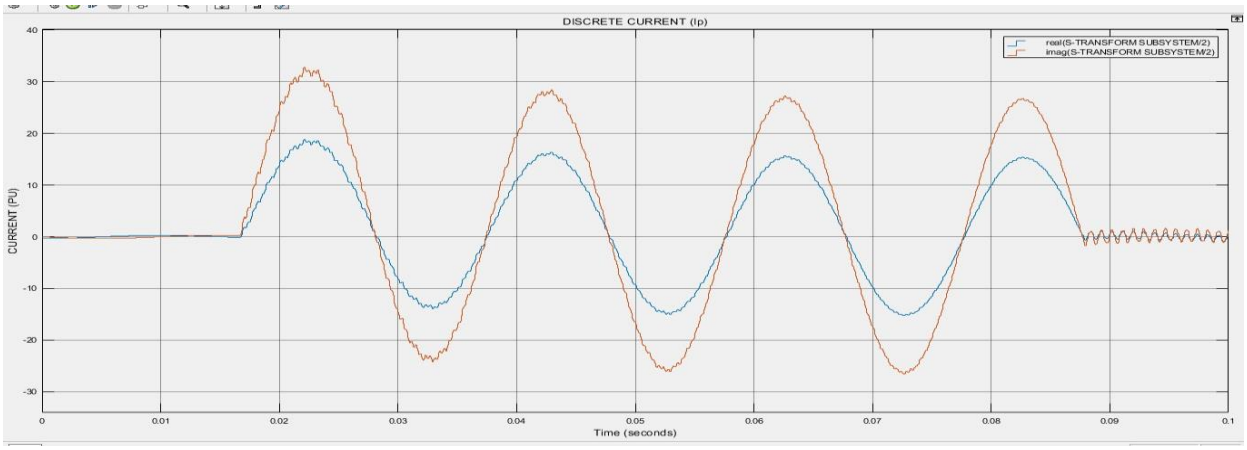

Figure 21: The Discrete Current Signal during Single Phase to Ground Fault Condition.

Table 4: The Result Obtained at Single Phase to Ground Fault Condition

S/N	PARAMETER	MAGNITUDE (PU)
1	Voltage (V)	0.4
2	Current (I)	40
3	Energy of the voltage signal E_j(J)	$1.7x10^{27}$
4	Energy of the current signal E_j (J)	$2.0x10^{30}$
5	S-transform of the voltage signal	$4x10^{13}$
6	S-transform of the current signal	$1x10^{15}$
7	Discrete voltage signal	1.0
8	Discrete current signal	20

iii. At Phase-to-Phase Fault Condition

The following findings were obtained when a phase-to-phase fault was simulated on the system, at a time of 17msecs and persisted until it was cleared at 94msecs, which lasted roughly 77msecs.

The current waveform reveals that once the fault arose, the faulty phase current magnitudes climbed to 120pu and persisted in this manner until the fault was cleared up. It was discovered that at the healthy phase, the amplitude of the current passing through it did not vary during the fault period. After the fault is resolved, the amplitude of the current in the faulty phases becomes uniform with the size of the current in the remaining healthy phase. Figure 23 shows the current waveform.

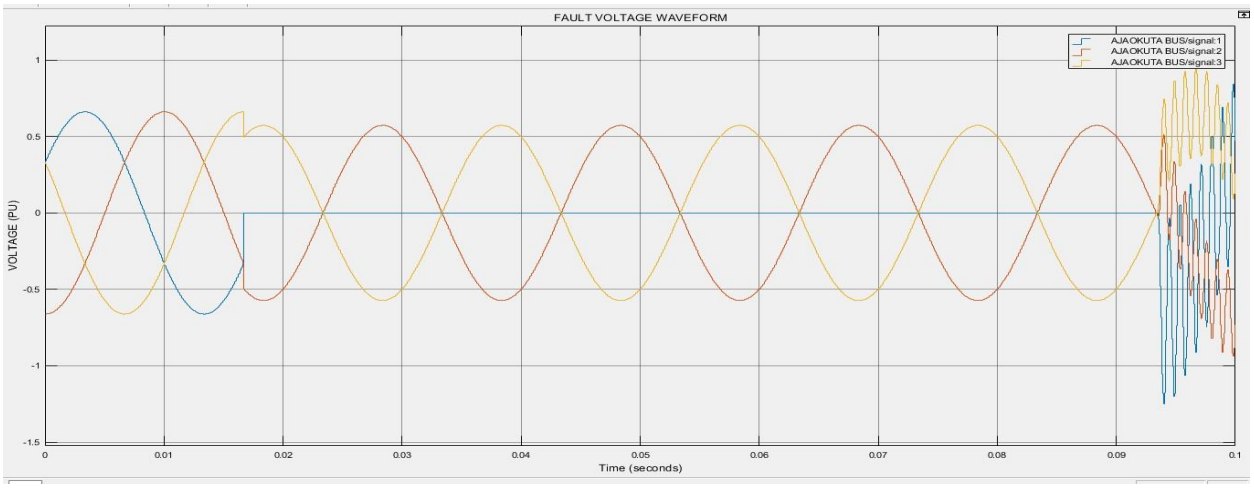

Figure 22: Phase to Phase Fault Voltage Waveform for the System Modelled.

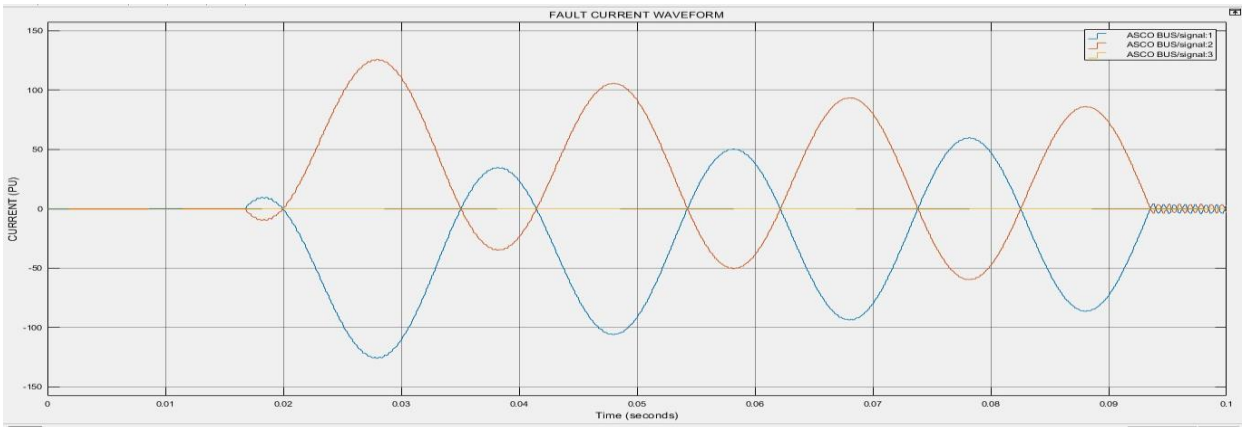

Figure 23: Phase to Phase Fault Current Waveform for the System Modelled.

Furthermore, the magnitude of the voltage energy signal from the S-Transform model in figure 24 gets distorted at $1.7x10^{27}J$ during the fault condition, which is now smaller than the size of the current energy signal in figure 25 at $2.7x10^{31}J$. When the fault occurs at 17msecs, the current energy signal magnitude spikes to $2.7x10^{31}J$ and is recovered once the fault is cleared at 94msecs.

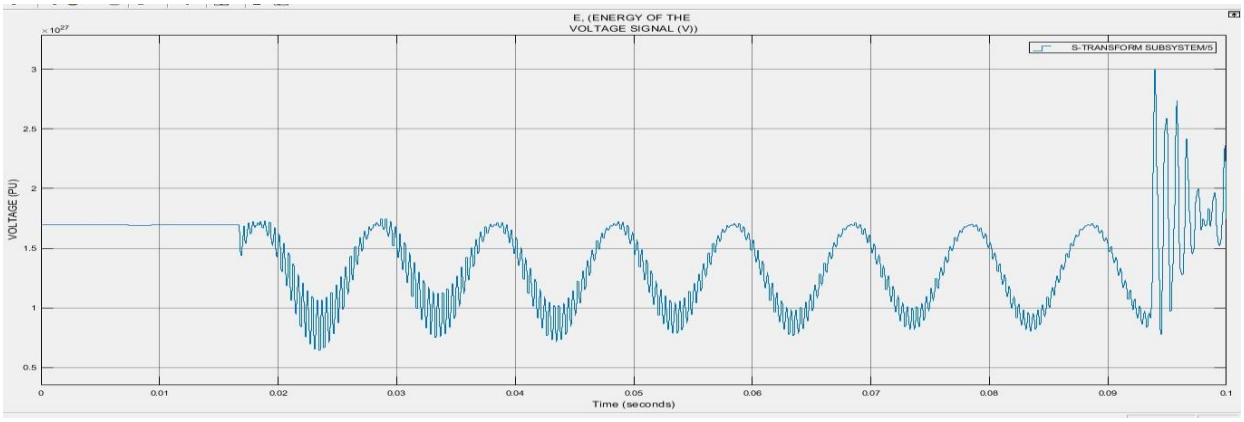

Figure 24: The Voltage Signal Energy Waveform during Phase-to-Phase Fault Condition.

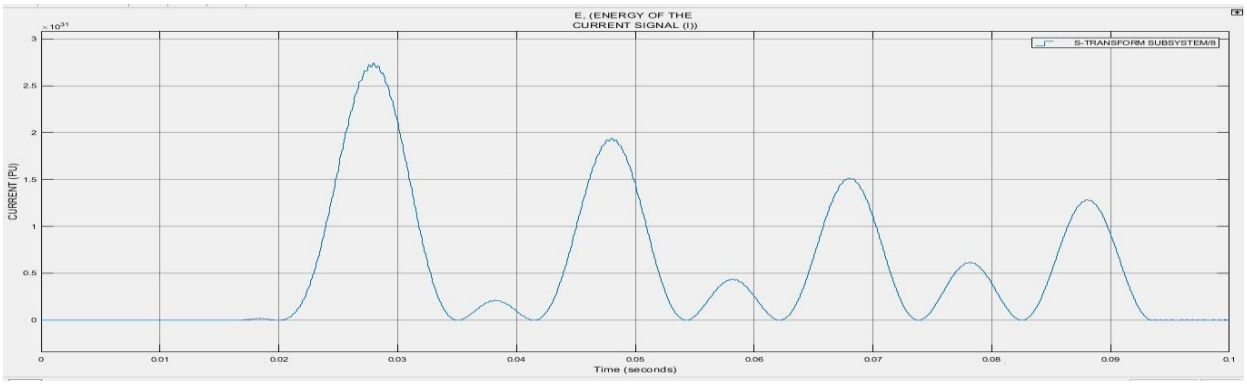

Figure 25: The Current Signal Energy Waveform during Phase-to-Phase Fault Condition.

Still also, the S-transform magnitude of the voltage signal from the S-Transform model in figure 26 gets distorted at $4x10^{13}$ during the fault condition, which is now smaller than the magnitude of the current signal in figure 27 at $1x10^{15}$. When the fault occurs at 17msecs, the current signal magnitude spikes to $1x10^{15}$ and is recovered once the fault is cleared at 85msecs.

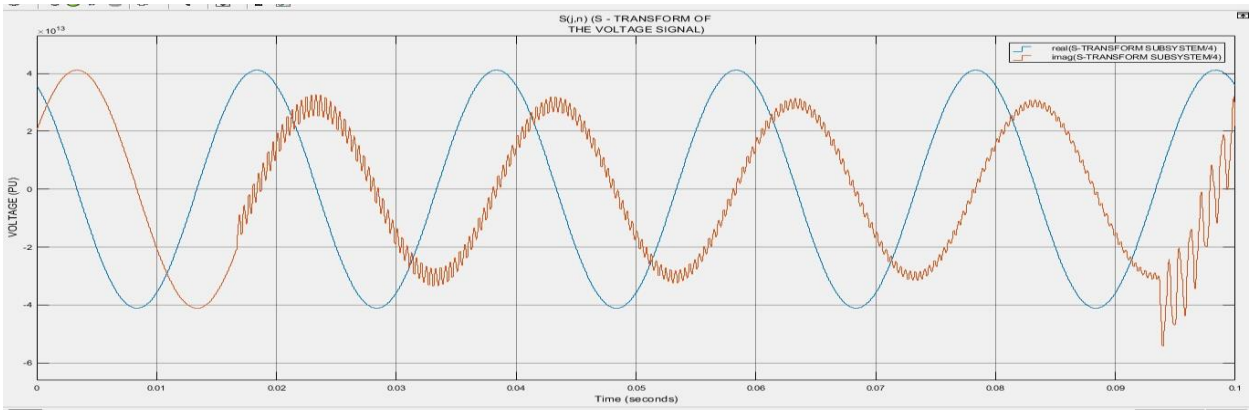

Figure 26: The S-transform of the Voltage Signal during Phase-to-Phase Fault Condition.

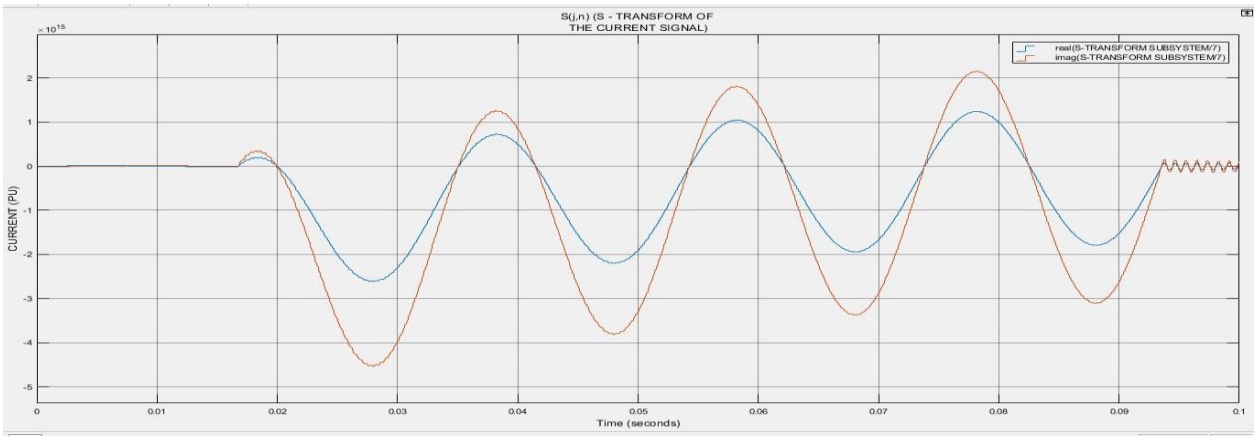

Figure 27: The S-transform of the Current Signal during Phase-to-Phase Fault Condition.

Finally, the discrete value of the voltage signal from the S-Transform model in figure 28 gets distorted at 1.0pu during the fault condition, which is now smaller than the discrete value of the current signal in figure 29 at 50pu. When the fault occurs at 17msecs, the current signal magnitude spikes to 50pu and is recovered once the fault is cleared at 85msecs.

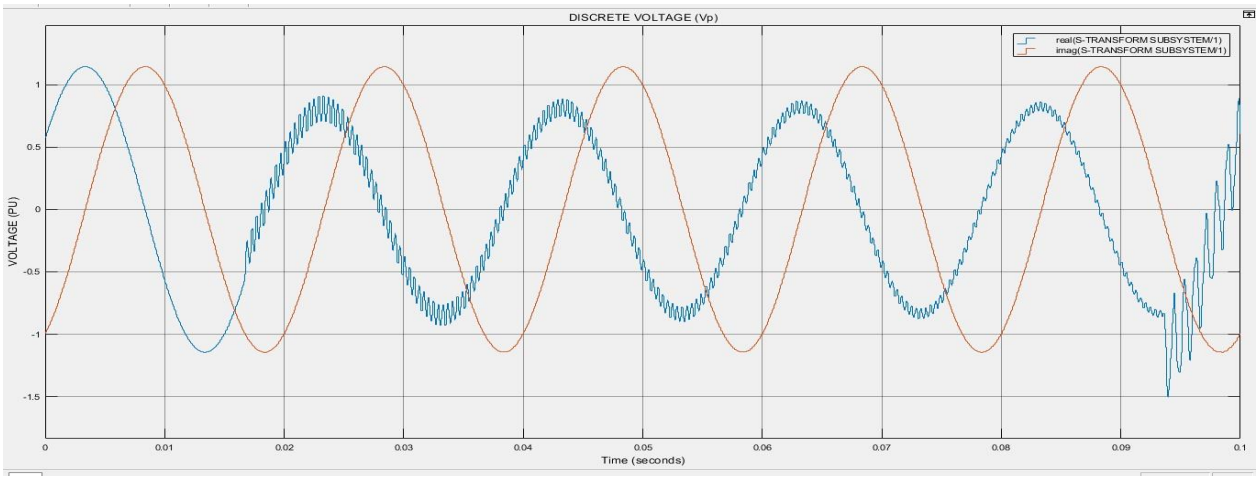

Figure 28: The Discrete Voltage Signal during Phase-to-Phase Fault Condition.

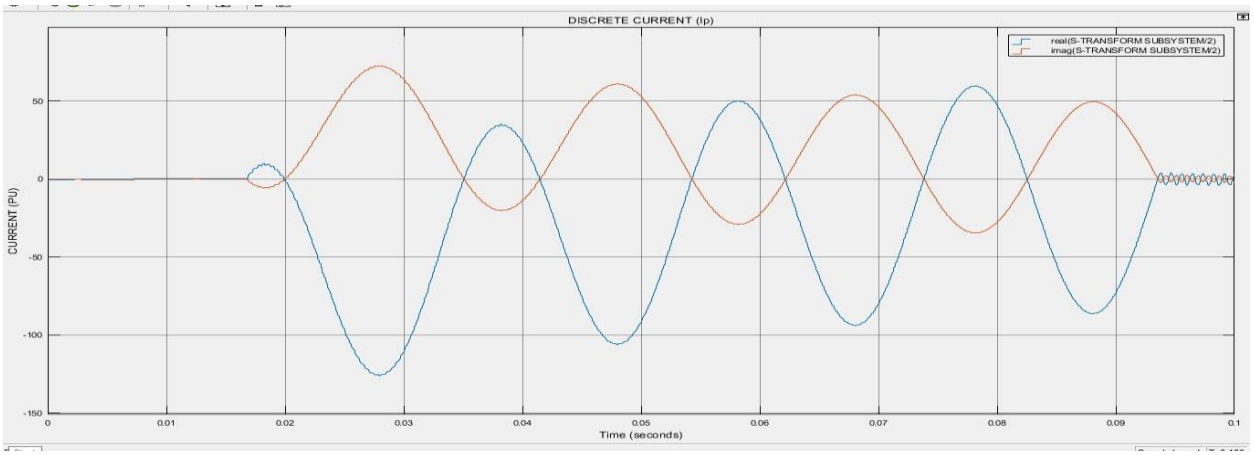

Figure 29: The Discrete Current Signal during Phase-to-Phase Fault Condition.

Table 5: The Result Obtained at Phase-to-Phase Fault Condition

S/N	PARAMETER	MAGNITUDE (PU)
1	Voltage (V)	0.5
2	Current (I)	120
3	Energy of the voltage signal E_j (J)	$1.7x10^{27}$
4	Energy of the current signal E_j (J)	$2.7x10^{31}$
5	S-transform of the voltage signal	$4x10^{13}$
6	S-transform of the current signal	$1x10^{15}$
7	Discrete voltage signal	0.1
8	Discrete current signal	50

iv. At Double Phase to Ground Fault Condition

The following data were obtained when a double phase to ground fault was begun on the system, at a time of 17msecs and persisted until it was cleared at 94msecs, which lasted roughly 77msecs.

The current waveform reveals that once the fault occurs, the faulty phase current magnitudes increase to 120pu for the double phase to ground fault and continue in this manner until the fault is removed. During the fault period, the amplitude of the current flowing through the healthy phase remained constant. After the fault is resolved, the amplitude of the current in the faulty phases becomes uniform with the size of the current in the remaining healthy phase. Figure 31 illustrates the current waveform.

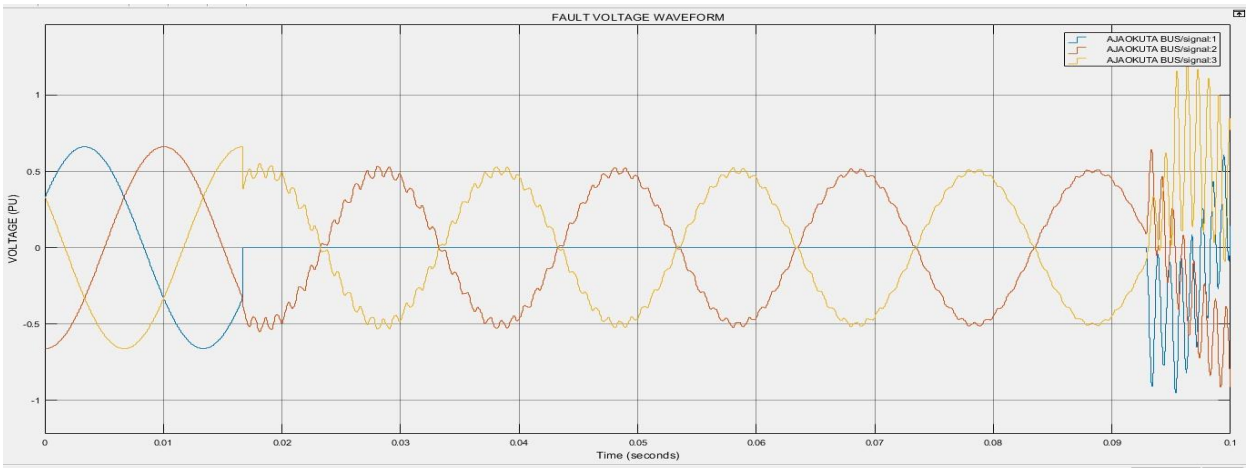

Figure 30: Double Phase to Ground Fault Voltage Waveform for the System Modelled.

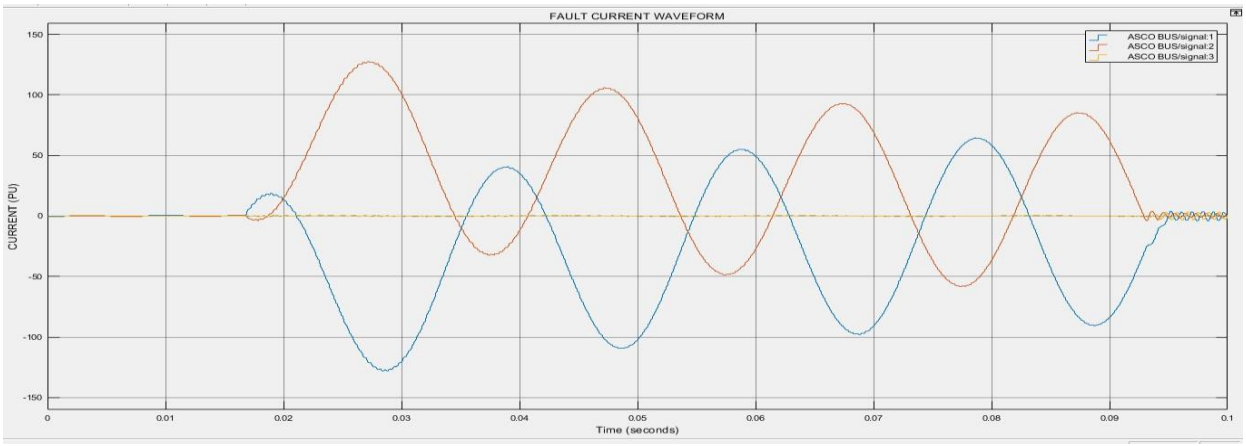

Figure 31: Double Phase to Ground Fault Current Waveform for the System Modelled.

Furthermore, the magnitude of the voltage energy signal from the S-Transform model in figure 32 gets distorted at $1.7x10^{27}J$ during the fault condition, which is now smaller than the size of the current energy signal in figure 33 at $2.7x10^{31}J$. When the fault occurs at 17msecs, the current energy signal magnitude spikes to $2.7x10^{31}J$ and is recovered once the fault is cleared at 94msecs.

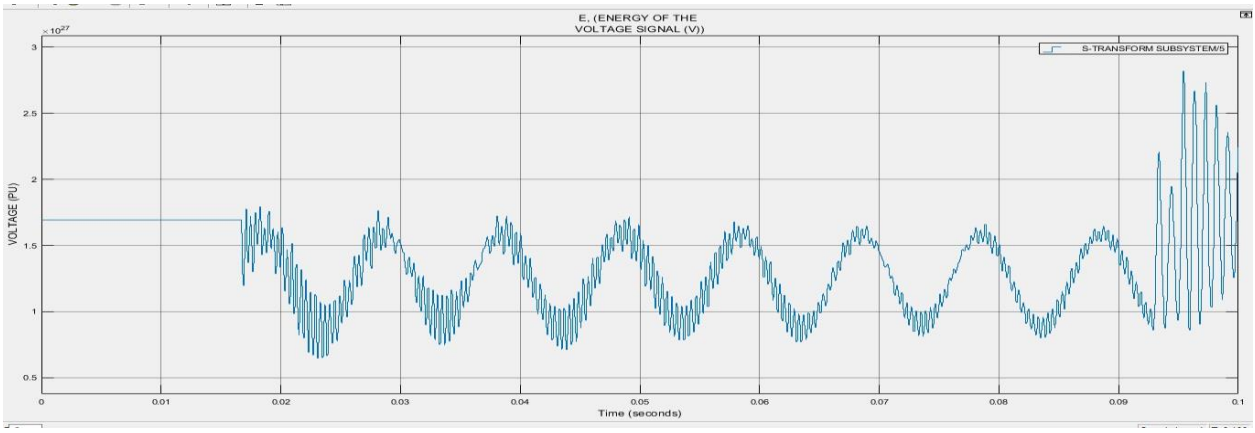

Figure 32: The Voltage Signal Energy Waveform during Double Phase-to-Ground Fault Condition.

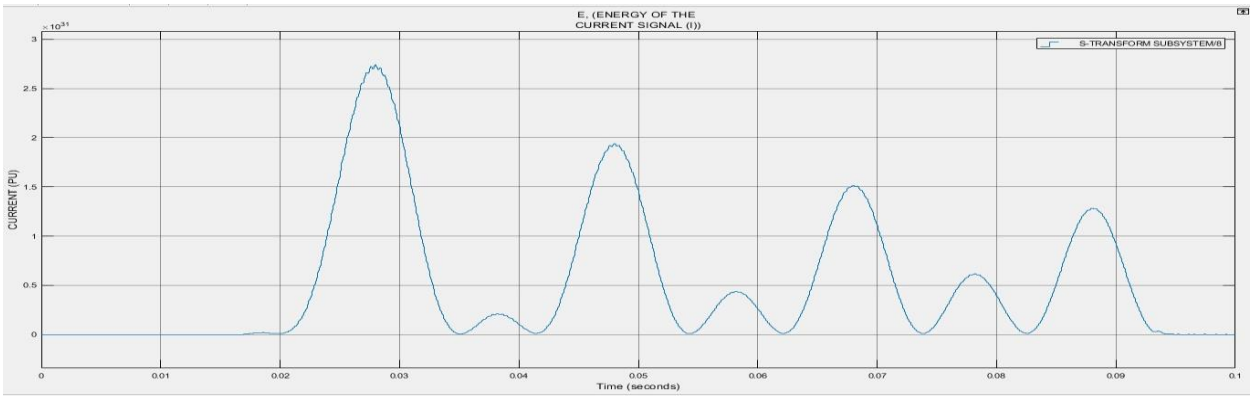

Figure 33: The Current Signal Energy Waveform during Double Phase-to-Ground Fault Condition.

Still also, the S-transform magnitude of the voltage signal from the S-Transform model in figure 34 gets distorted at 4x10e13 during the fault condition, which is now smaller than the magnitude of the current signal in figure 35 at 2x10e15. When the fault occurs at 17msecs, the current signal magnitude spikes to 1x10e15 and is recovered once the fault is cleared at 85msecs.

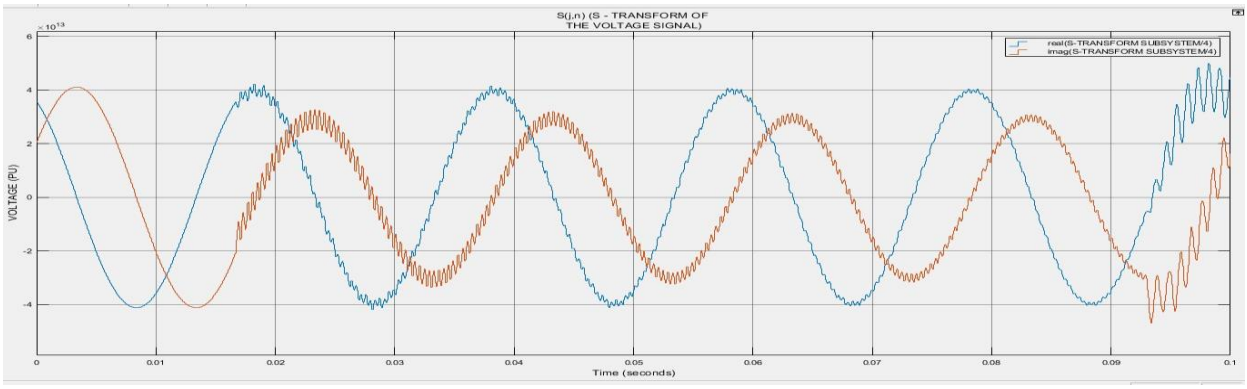

Figure 34: The S-transform of the Voltage Signal during Double Phase-to-Ground Fault Condition.

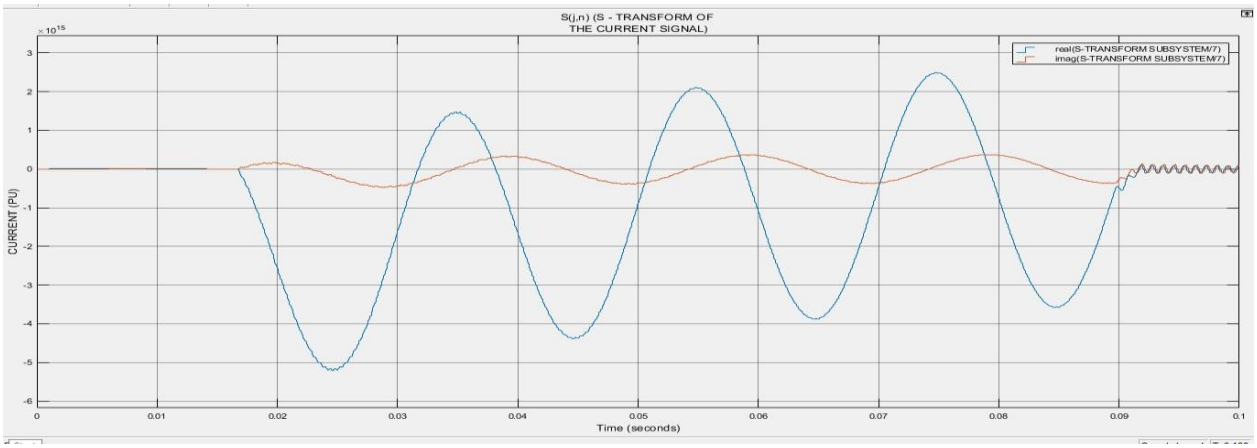

Figure 35: The S-transform of the Current Signal during Double Phase-to-Ground Fault Condition.

Finally, the discrete value of the voltage signal from the S-Transform model in figure 36 gets distorted at 1.0pu during the fault condition, which is now smaller than the discrete value of the current signal in figure 37 at 150pu. When the fault occurs at 17msecs, the current signal magnitude spikes to 150pu and is recovered once the fault is cleared at 85msecs.

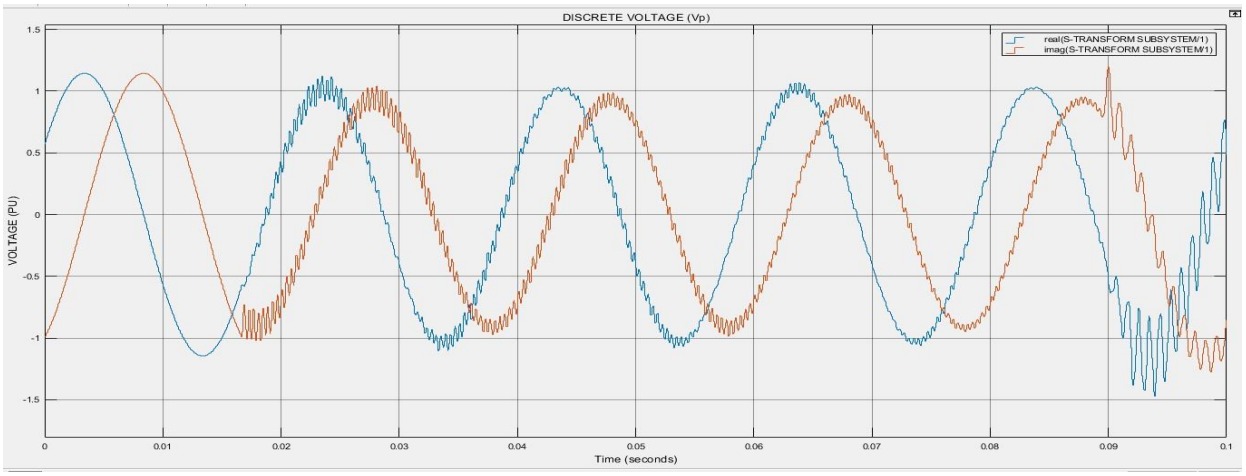

Figure 35: The Discrete Voltage Signal during Double Phase-to-Ground Fault Condition.

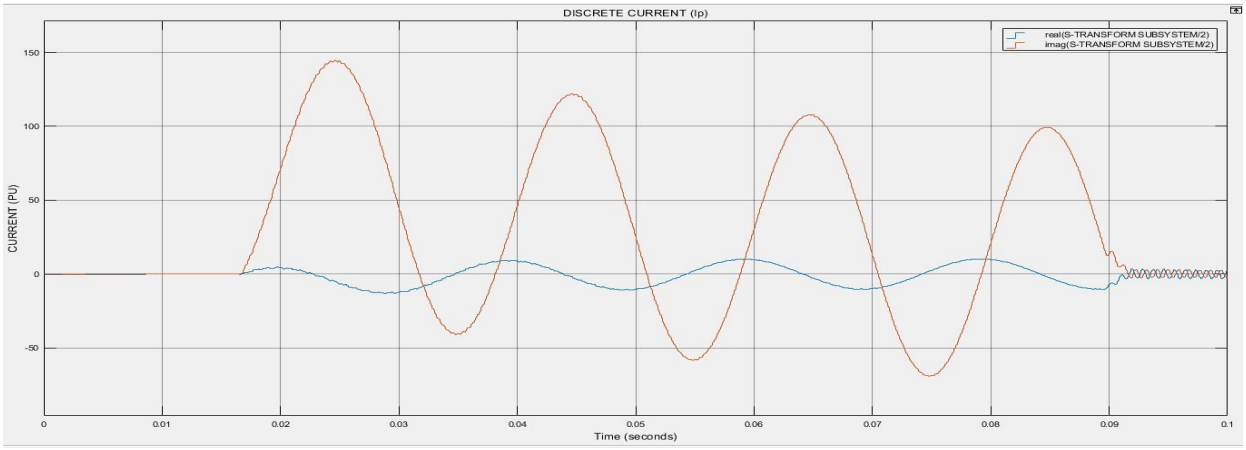

Figure 37: The Discrete Current Signal during Double Phase-to-GroundFault Condition.

Table 6: The Result Obtained at Double Phase-to-Ground Fault Condition

S/N	PARAMETER	MAGNITUDE (PU)
1	Voltage (V)	0.5
2	Current (I)	120
3	Energy of the voltage signal E_j (J)	$1.7x10^{27}$
4	Energy of the current signal E_j (J)	$2.7x10^{31}$
5	S-transform of the voltage signal	$4x10^{13}$
6	S-transform of the current signal	$2x10^{15}$
7	Discrete voltage signal	0.1
8	Discrete current signal	150

v. At Three Phase Fault Condition

On simulation of a three-phase fault condition. Figure 38 depicts the voltage waveform. When the fault was triggered, the three-phase voltage dropped from 0.6 to zero at 17msecs and persisted until the fault was cleared at 85msecs before it was restored. This lasted 68 msecs.

When the three-phase fault was initiated at 17msecs, the current value rose to roughly 130pu for phase A, 150pu for phase B, and 130pu for phase C. This pattern continued until the fault was cleared at 90ms and the current waveform reverted to its initial point of zero. This is clearly seen in figure 39.

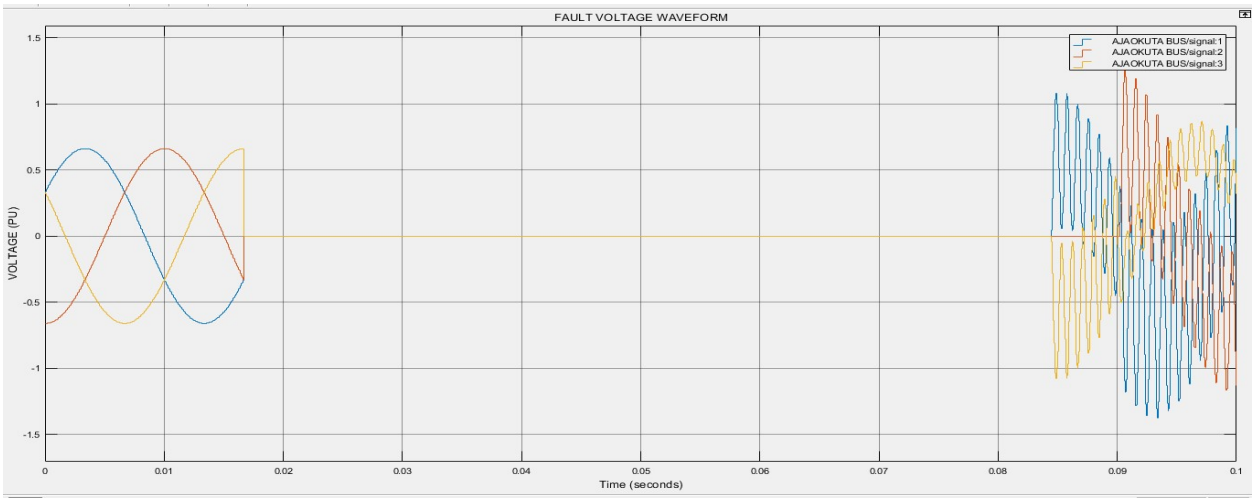

Figure 38: Three Phase Fault Voltage Waveform for the System Modelled.

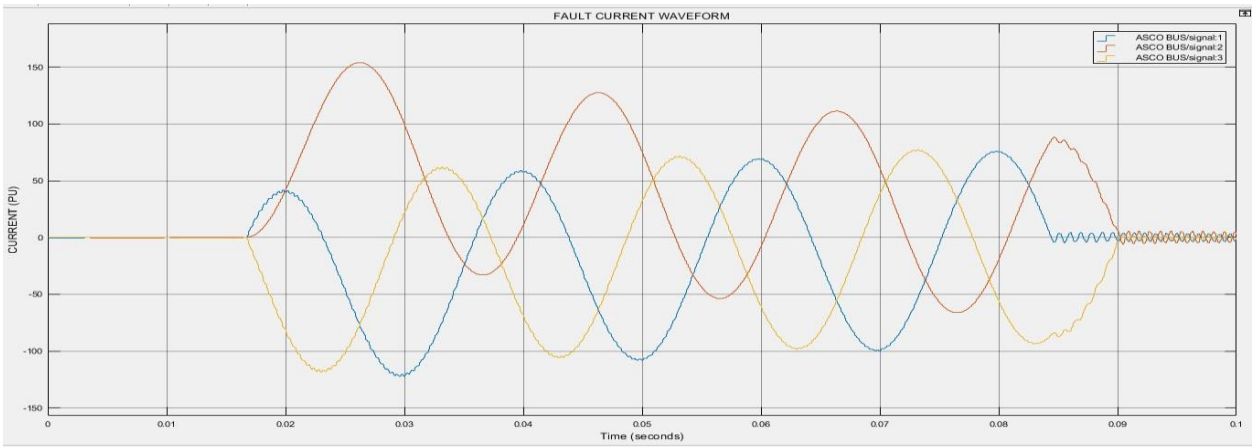

Figure 39: Three Phase Fault Current Waveform for the System Modelled.

Furthermore, the magnitude of the voltage energy signal from the S-Transform model in figure 40 gets distorted and lowers to $1.7x10^{27}J$ during the fault scenario, which is now smaller than the magnitude of the current energy signal in figure 41, which is $3.1x10^{31}J$. When the fault occurs at 17msecs, the current energy signal magnitude spikes to $3.1x10^{31}J$ and is recovered once the fault is cleared at 90msecs.

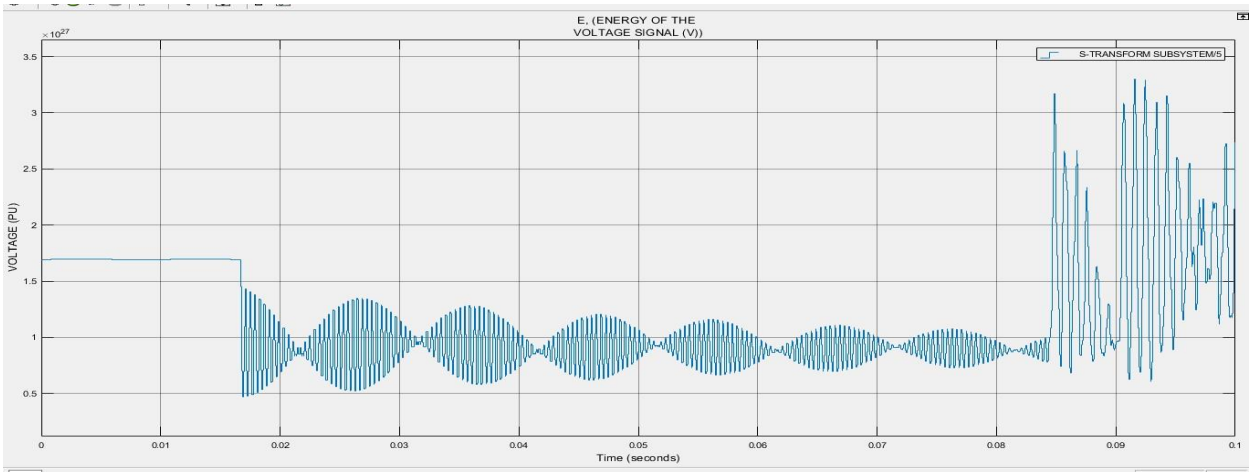

Figure 40: The Voltage Signal Energy Waveform during Three Phase Fault Condition.

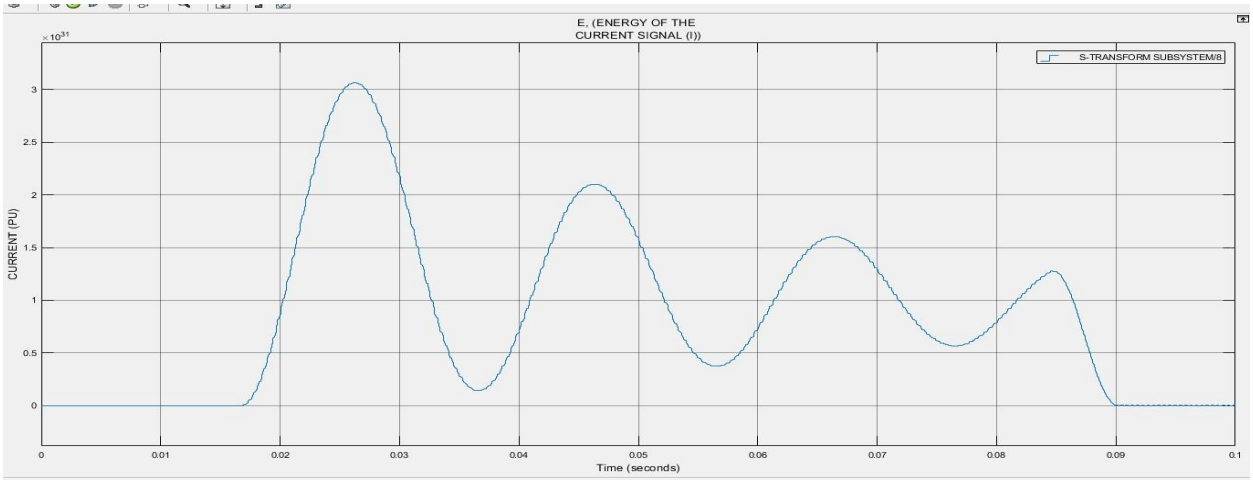

Figure 41: The Current Signal Energy Waveform during Three Phase Fault Condition.

Still also, the S-transform magnitude of the voltage signal from the S-Transform model in figure 42 gets distorted at $4x10^{13}$ during the fault condition, which is now smaller than the magnitude of the current signal in figure 43 at $3x10^{15}$. When the fault occurs at 17msecs, the current signal magnitude spikes to 1x10e15 and is recovered once the fault is cleared at 85msecs.

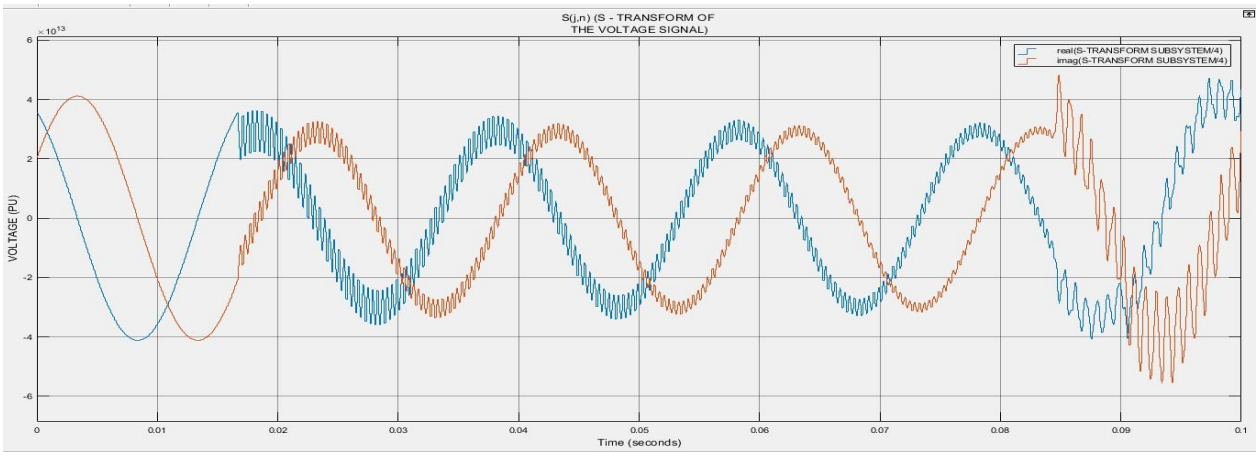

Figure 42: The S-transform of the Voltage Signal during Three Phase Fault Condition.

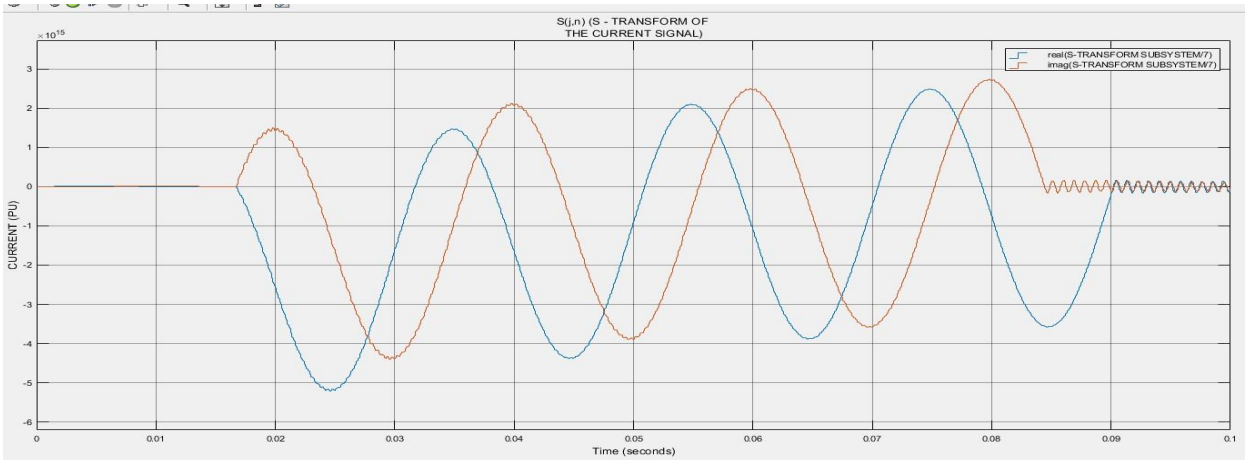

Figure 43: The S-transform of the Current Signal during Three Phase Fault Condition.

Finally, the discrete value of the voltage signal from the S-Transform model in figure 44 gets distorted at 1.0pu during the fault condition, which is now smaller than the discrete value of the current signal in figure 45 at 150pu. When the fault occurs at 17msecs, the current signal magnitude spikes to 150pu and is recovered once the fault is cleared at 85msecs.

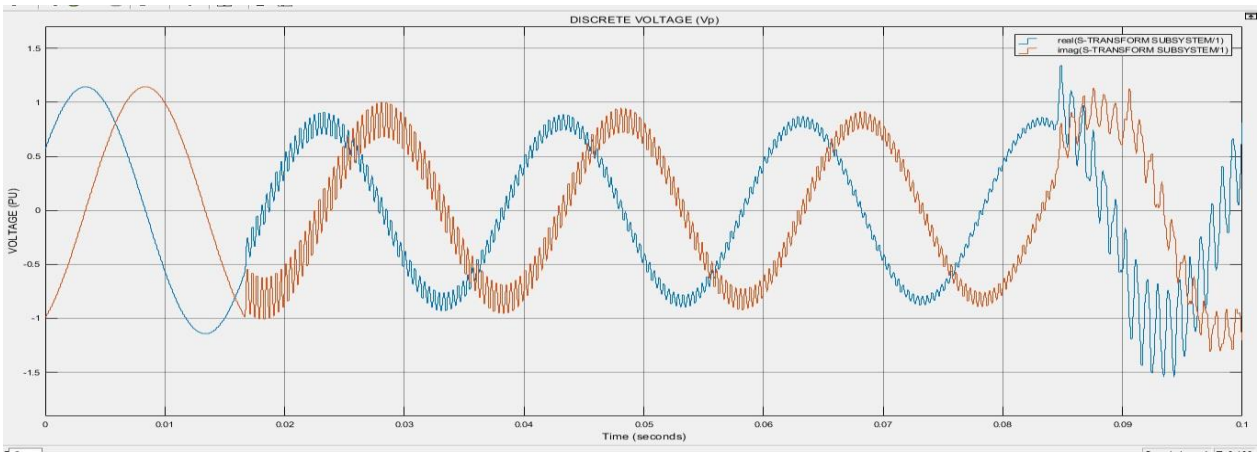

Figure 44: The Discrete Voltage Signal during Three Phase Fault Condition.

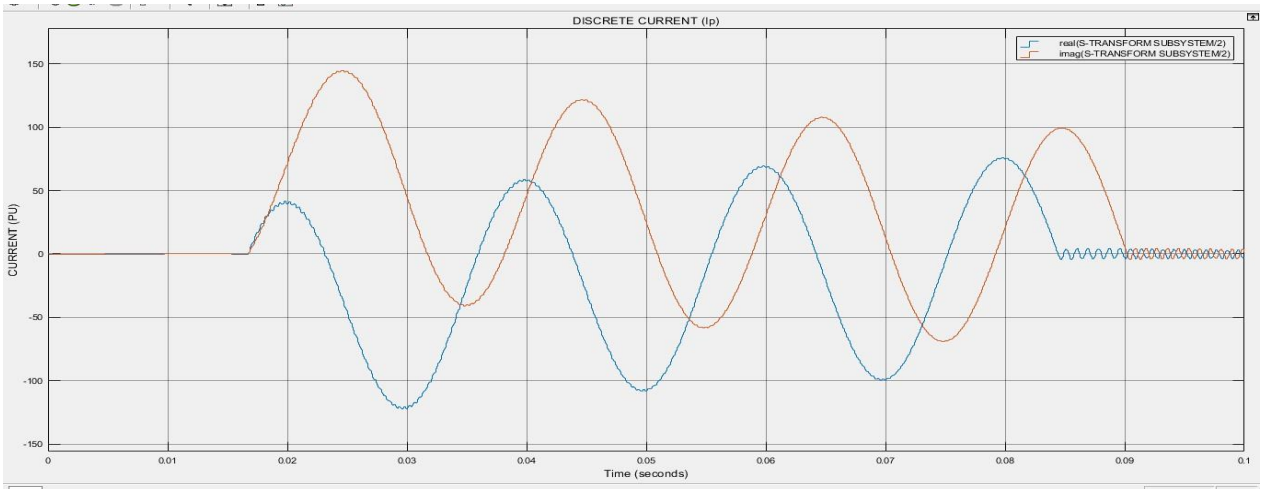

Figure 45: The Discrete Current Signal during Three Phase Fault Condition.

Table 7: The Result Obtained at Three Phase Fault Condition

S/N	PARAMETER	MAGNITUDE (PU)
1	Voltage (V)	0.65
2	Current (I_a)	130
3	Current (I_b))	150
4	Current (I_c))	130
5	Energy of the voltage signal E_j (J)	$1.7x10^{27}$
6	Energy of the current signal E_j (J)	$3.1x10^{31}$
7	S-transform of the voltage signal	$4x10^{13}$
8	S-transform of the current signal	$3x10^{15}$
9	Discrete voltage signal	0.1
10	Discrete current signal	150

4.0. Conclusion

The dependability of electric power transmission system is highly impacted by the presence of fault in the system. This study on "fault diagnosis of a 330kv Ajaokuta-Lokoja 47.39km transmission line using S-Transform technique addressed this objective by sampling the fault voltage and current transient on the transmission line at relay point. The fault generated voltage and current signals at various faults condition were diagnose using the voltage and current energy signal, the S-transform waveform, and the discrete voltage and current signal. At pre-fault condition, the energy of the voltage signal $1.6947x10^{27}J$ was greater than that of the energy of the current signal $1.2725x10^{26}J$, the S-Transform of the voltage signal was $4x10^{13}$ while the S-Transform of the current signal was $1x10^{13}$ and the discrete voltage signal was at 1.0pu while the discrete current signal wat at 0.3pu. which all were in accordance with conventional circuit theorem. At various fault conditions say single phase to ground fault, the energy of the voltage was $1.7x10^{27}J$ while the energy of the current signal was $2.0x10^{30}J$, the S-Transform of the voltage signal was $4x10^{13}$ while the S-Transform of the current signal was $1x10^{15}$ and the discrete voltage signal was at 1.0pu while the discrete current signal was at 20p.u. As seen, the value of the current magnitude was greater than the values of the voltage magnitude at each fault condition accordance with conventional circuit theorem.

This research has been able to present a fault diagnosis method for grid operators to be able to detect and diagnose various fault that will occur in the transmission line system which will have a significant impact on the system reliability as the longer it takes for the fault to be cleared, the less reliable the system is and vice versa.

References

Anazia, E.A., Ogboh V.C. and Anionovo, U.E., 2020. Time-frequency analysis technique for fault investigation on power system transmission lines. *International journal of engineering inventions, e-ISSN: 2278-7461, p-ISSN: 2319-6491. Volume 9, issue 6, PP: 18-25, 21 August, 2020.*

Haroun, S., Seghir, A.N. and Touati, S.J., 2018. Multiple feature extraction and selection for detection and classification of stator winding faults. *IET electrical power application, 12(3), 339-346, 08 March, 2022.*

Iwuamadi, O.C., Ezechukwu, O.A. and Ogboh, V.C., 2022. Application of S-Transform for fault studies on 330kV transmission line. *American journal of engineering research (AJER), 11(01), 75-98. Retrieved from www.ajer.org on 27 March, 2023.*

Jose, J.C., Marjan, P., David, L., Sadegh, A. and Vladimir, T. (2021). S-Transform based fault detection algorithm for enhancing distance protection performance. *International journal of electrical power and energy systems, 130, 1-9. Doi: 10.1016/j.ijepes.2021.106966, 14 March, 2022.*

Kunjin, C., Caowei, H. and Jinliand, H. (2016). Fault detection, classification and location for transmission lines and distribution systems: a review on the methods. *High volt., vol 1 iss, pp. 25-33. Doi: 10.1049/hve.2016.0005. www.ietdl.org. 2016*

Mahmoud, R.A. (2022) Simple algorithm for fault detection, classification and direction discrimination in power systems based on digital current signal processing. *J. Eng. 2022, 478-511. https://doi.org/10.1049/tje2.12131. 2022*

Mohamed, A., Abidin, A.F. and Shareef, H., 2014. Intelligent detection of unstable power swing for correct relay operation using S-Transform and neural networks. *Expert systems with applications, vol. 38, pp. 14969-14975, 2011.*

Raza, A., Benrabah, A., Alquthami, T. and Akmal, M. (2020). A review of fault diagnosing methods in power transmission systems. *Applied science, 10(4), 1312. Doi: 10.3990/app10041312, 04 March, 2022.*

Shafiullah, M., Abido, M. and Al-Mohammed, A., 2022. Advanced signal processing techniques for feature extraction. *Power system fault diagnosis. Pp. 101-120. Doi: 10.1016/B978-0-323-88429-7-00001-1, January, 2022.*

Shafiullah, M. (2024). Fault diagnosis in distribution grids under load and renewable energy uncertainties. *Retrieved fromhttps://www.researchgate.net/publication/359931773_Fault_Diagnosis_in_Distribution_Grids_under_Load and_Renewable_Energy_Uncertainties. On 22 January, 2024.*

Stockwell, R.G., Mansinha, L. and Lowe, R.P., 1996. Localization of the complex spectrum: The S-transform. *IEEE transactions on signal processing, 44(4), 998-1001. Doi: 10.1109/78.492555, 13 March, 2022*